ELSEVIER

Quaternary Science Reviews 24 (2005) 1063–1081

QSR

Patterns of deglacial warming in the Pacific Ocean: a review with emphasis on the time interval of Heinrich event 1

T. Kiefer[a,*], M. Kienast[b,1]

[a]Department of Earth Sciences, University of Cambridge, Downing Street, Cambridge CB2 3EQ, UK
[b]Woods Hole Oceanographic Institution, Woods Hole, MA, 02543, USA

Received 10 September 2003; accepted 25 February 2004

Abstract

Based on a compilation of currently available records of past sea surface temperature (SST) variability, estimated from a variety of different proxies, the regional-scale deglacial SST development in the Pacific Ocean is tentatively classified into four endmember types. The subtropical and tropical Pacific is characterized by a continuous deglacial warming without marked interruption during the time interval of Heinrich event 1 (H1), whereas the subarctic North Pacific exhibits centennial-scale warm-cold oscillations during this time interval. SST records from marginal seas of the Pacific show a deglacial warming interrupted by a cooling event coeval with H1, followed by a marked Bølling SST increase. A single SST record from the southwestern subantarctic Pacific displays a continuous deglacial warming across H1 followed by an Antarctic Cold Reversal-type cooling during the Allerød. Thus, in contrast to the deglacial SST development in the Atlantic, which has been inferred to be overwhelmingly driven by the redistribution of heat through changes in the meridional overturning circulation (MOC), none of the open oceanic Pacific SST records reviewed here displays any obvious and/or dominant response to the reduction of the MOC and/or the reorganization of atmospheric circulation during H1. Within the limits of absolute chronologies, all tropical and subtropical Pacific SST records show an onset of deglacial warming at 19 ± 1 ka, coeval with the onset of the deglacial rise in sea level.

1. Introduction

The transition from the last glacial maximum to the Holocene is punctuated by various high-frequency oscillations, for example the Bølling warm phase, the Heinrich event 1 (H1) and Younger Dryas (YD) cold periods, or the Antarctic Cold Reversal (ACR). These oscillations may not have been global in extent, and their geographic distribution is still a matter of considerable debate (see for example Broecker and Hemming, 2001; Clark et al., 2002). For the Atlantic Ocean an asynchronous development of deglacial SST between the northern and southern hemisphere is suggested in some records (e.g., Rühlemann et al., 1999; Vidal et al., 1999; see Clark et al., 2002 for a comprehensive review), supporting the concept of the bipolar seesaw (Crowley, 1992; Broecker, 1998; Alley and Clark, 1999; Stocker, 2000; for a different view see Morgan et al., 2002). According to the seesaw hypothesis, a decrease/cessation of the southward flux of North Atlantic Deep Water is accompanied by a decrease in northward heat transport in the Atlantic, which, in turn, leads to an accumulation of heat in the tropical Atlantic, the South Atlantic, and the Southern Ocean. Conversely, a vigorous North Atlantic Deep Water flux extracts heat from these latter regions.

Irrespective of whether one accepts a northern (e.g., Alley et al., 2002) or a southern (e.g., Petit et al., 1999) hemisphere lead of the deglacial warming, or a synchroneity of both (e.g., Steig et al., 1998; Grootes

*Corresponding author. Tel.: +44-1223-333442; fax: +44-1223-333450
E-mail address: tkie02@esc.cam.ac.uk (T. Kiefer).
[1]Now at: Department of Oceanography, Dalhousie University, Halifax, NS, Canada.

0277-3791/$ - see front matter © 2004 Elsevier Ltd. All rights reserved.
doi:10.1016/j.quascirev.2004.02.021

et al., 2001), it is evident that the deglacial warming trend in the circum-North Atlantic realm was temporarily suppressed during H1. Thus, H1 is both associated with a significant cooling in the North Atlantic (Bond et al., 1992; Bard et al., 2000), with the most pronounced reduction of the MOC during the last 30 kyr (e.g. Sarnthein et al., 1994; McManus et al., 2004), as well as with a reorganization of atmospheric circulation (e.g., Porter and An, 1995; Wang et al., 2001; Rohling et al., 2003). As such, H1 represents a major perturbation of the climate system, and mapping its regional manifestation will further our understanding of mechanistic linkages between different components of the climate system, as well as of the communication of climate signals between distant regions.

Current model simulations of SSTs in the Pacific Ocean in response to a collapse of the MOC show conflicting results. For example, the simulations examined by Manabe and Stouffer (1995), Schiller et al. (1997); see also Mikolajewicz et al. (1997), and Vellinga and Wood (2002) all show a significant cooling in the North Pacific as a result of a MOC shutdown. In contrast, the simulations of Huang et al. (2000) as well as of Weaver et al. (1999) and Schmittner et al. (2003) predict a subtle warming throughout the Pacific. This discrepancy could be partly due to the fact that usually only snapshots in time are displayed in these presentations, aimed at highlighting features in the Atlantic Ocean rather than integrated averages of the dynamic response in the Pacific to a collapse of the MOC. Furthermore, all these modelling studies tend to be meltwater experiments on modern boundary conditions, and they are based on the a priori assumption that the climatic signal during H1 originates in the North Atlantic. All these models do agree, however, in predicting only very minor changes in tropical Pacific SSTs in response to a collapse of the MOC.

Here we review deglacial Pacific SST records in an attempt to evaluate the impact of H1 on the deglacial SST development in the Pacific Ocean (for a definition of H1 see below). We further aim to establish regional differences and commonalities of the deglacial SST rise in the Pacific Ocean, and to examine potential mechanistic linkages.

2. Approach

In this review, only SST records with high resolution and with independent radiocarbon chronologies are considered for defining deglacial SST patterns (Table 1, Fig. 1). Radiocarbon chronologies are essential because lead-lag relations with respect to planktonic foraminiferal $\delta^{18}O$ could be obscured by changes in sea surface salinities, which have been shown to be significant, particularly during the deglaciation (e.g. Rosenthal et al., 2003). For the same reason, we do not include SST reconstructions based solely on foraminiferal $\delta^{18}O$. However, in order to increase the data coverage throughout the Pacific, and in line with the MARGO (Multiproxy Approach for the Reconstruction of the Glacial Ocean surface) strategy, we incorporate SST records from different proxies, namely alkenone unsaturation index, Mg/Ca ratio, and foraminiferal and dinocyst assemblages (Table 1, Fig. 1), even though this direct comparison of SST records derived from different proxies might impose significant distortions to our interpretations. This approach is justified, however, by the fact that a number of Pacific sites where deglacial SSTs have been reconstructed using different proxies show an overall agreement between all methods used (see further discussion below). Furthermore, none of our conclusions is based on a single record or records using a single SST proxy.

The SST records were adopted as published by the authors, making no attempt to harmonize the data towards any particular calibration or method. This approach imposes a focus on the main features of the deglacial rise in SST, thereby largely ignoring absolute temperatures or temperature gradients.

Given the fact that both the atmospheric transport of the temperature signal as well as the impact of changes in the strength of the MOC should be felt almost instantaneously around the globe we do not attempt to evaluate decadal to centennial lead-lag features or whether H1 is the result of the transmission of paleoclimate signals from the North Atlantic elsewhere or whether they are due to a common forcing ('joint dependency', Clark and Bartlein, 1995). Instead, we classify patterns of similar SST evolution across the deglaciation, thereby generally tolerating deviations in the timing of events on the order of several centuries to one millennium. This is considered to approximate the actual precision of most radiocarbon-based age constraints for Pacific sediment cores, which are limited by the (usually small) analytical error of the ^{14}C dates, errors and uncertainties in the paleo-reservoir ages (Sikes et al., 2000; Kovanen and Easterbrook, 2002; Kienast et al., 2003), and errors and uncertainties in the relationship between ^{14}C ages and calendar ages beyond the tree-ring calibration (Stuiver et al., 1998).

By definition, Heinrich events are restricted to the North Atlantic. Accordingly, any assessment of climate change outside the North Atlantic during or in response to Heinrich events has to resort to defining a time period that is equivalent to these North Atlantic events. Thus, for the purpose of this review H1 is defined as the time interval 17.5–14.7 ka. Even though this broad period possibly extends beyond the time of the actual deposition of detrital layers in the North Atlantic (François and Bacon, 1994; but see also Elliot et al., 1998; Clarke et al., 1999; Veiga-Pires and Hillaire-Marcel, 1999;

Table 1
Core sites in the Pacific with deglacial records of sea surface temperature (SST). Deglacial SST patterns are labelled 'A'–'D' as in Fig. 6. Sedimentation rates (SR) are given for the deglacial interval (ca 19–11 cal ka).

Core	Region	Latitude	Longitude	Water depth (m)	Age constraint	SR (cm/kyr)	SST Proxies	SST pattern	Reference
Core sites with deglacial SST records reviewed in this study									
PAR87A-10	Subarctic NE Pacific	54.36	−148.47	3664	^{14}C ages	11	Dinocysts, Radiolaria	C	de Vernal and Pedersen (1997); Sabin and Pisias (1996)
MD01-2416	Subarctic NW Pacific	51.27	167.73	2317	^{14}C ages/^{14}C plateau	10–34	Mg/Ca, PF	C	Kiefer et al. submitted
ODP Site 883	Subarctic NW Pacific	51.20	167.77	2385	^{14}C ages/^{14}C plateau	10–28	Mg/Ca, PF	C	Kiefer et al. submitted
JT96-09	Subarctic NE Pacific	48.91	−126.89	920	^{14}C ages	63	$U^{K'}_{37}$	C?	Kienast and McKay (2001)
W8709A-8TC	Subarctic NE Pacific	42.50	−127.68	3111	^{14}C ages	9	$U^{K'}_{37}$, radiolaria	C	Prahl et al. 1995; Sabin and Pisias (1996)
ODP 1019	California margin	41.68	−124.93	980	^{14}C ages	63	$U^{K'}_{37}$, Np coiling ratios	C?	Barron et al. (2003); Mangelsdorf et al. (2000); Mix et al. (1999)
ODP 1017	California margin	34.53	−120.89	955	^{14}C ages	19	$U^{K'}_{37}$	C	Seki et al. (2002); Mangelsdorf et al. (2000)
ODP 893	California margin	34.29	−120.04	575	^{14}C ages	170	PF	D	Hendy et al. (2002)
PC17	Subtropical Pacific	21.36	−158.19	503	^{14}C ages	2.5	$U^{K'}_{37}$, PF	A	Lee et al. (2001); Lee and Slowey 1999
17940	South China Sea	20.12	117.38	1727	^{14}C ages/benthic δ^{18}O	21–76	$U^{K'}_{37}$, PF	D	Pelejero et al. (1999); Pflaumann and Jian (1999)
SO50-31KL	South China Sea	18.76	115.87	3360	^{14}C ages	10	$U^{K'}_{37}$, PF	D?	Huang et al. (1997b); Chen and Huang (1998)
SCS90-36	South China Sea	18.00	111.49	2050	^{14}C ages	6	$U^{K'}_{37}$, PF	D?	Huang et al. (1997a)
18252	South China Sea	9.23	109.38	1273	^{14}C ages	70	$U^{K'}_{37}$	D	Kienast et al. (2001)
MD97-2151	South China Sea	8.73	109.87	1589	^{14}C ages	23	$U^{K'}_{37}$, PF	D	Huang et al. (2002)
MD97-2141	Sulu Sea	8.80	121.30	3633	^{14}C ages	22	Mg/Ca	A	Rosenthal et al. (2003)
MD98-2181	W tropical Pacific	6.30	125.83	2114	^{14}C ages	48	Mg/Ca	A	Stott et al. (2002)
17964	South China Sea	6.16	112.21	1556	^{14}C ages	46	$U^{K'}_{37}$	D	Pelejero et al. (1999)
18287	South China Sea	5.65	110.65	598	^{14}C ages	55	$U^{K'}_{37}$, PF, Mg/Ca	D	Steinke et al. (2001); Whitko et al. (2002)
TR163-19	E equatorial Pacific	2.26	−90.95	2348	^{14}C ages	4	Mg/Ca	A	Lea et al. (2000); Spero and Lea (2002)
V21-30	E equatorial Pacific	−1.22	−89.68	617	^{14}C ages	15	Mg/Ca	A	Koutavas et al. (2002)
ERDC-92	Central equat. Pacific	−2.23	157.00	1598	^{14}C ages	1–2.5	Mg/Ca	A	Palmer and Pearson (2003)
MD98-2162	W equatorial Pacific	−4.69	117.90	1855	^{14}C ages	33	Mg/Ca	A	Visser et al. (2003)
17748-2/ GeoB3302-1	SE Pacific	−33.22	−72.10	1498	^{14}C ages	13–66	$U^{K'}_{37}$	A	Kim et al. (2002)
MD97-2120	SW Pacific	−45.53	174.93	1210	^{14}C ages	13–22	Mg/Ca	B	Pahnke et al. (2003)
Core sites with lack of independent age control, very low resolution, or inferred dominance of localized SST variability									
TT39-PC12	NE Pacific	49.41	−128.19	2369	^{14}C ages on bulk organic C	ca. 15	Radiolaria		Sabin and Pisias (1996)
TT39-PC17	NE Pacific	48.23	−130.01	2795	^{14}C ages on bulk organic C	ca. 20	Radiolaria		Sabin and Pisias (1996)

Table 1 (*continued*)

Core	Region	Latitude	Longitude	Water depth (m)	Age constraint	SR (cm/kyr)	SST Proxies	SST pattern	Reference
V20-120	Subarctic NW Pacific	47.40	167.75	6216	radiolaria abundance	ca. 3	Radiolaria		Heusser and Morley (1997)
EW9504-17PC	NE Pacific	42.24	−125.89	2671	few ^{14}C ages	28	Radiolaria		Pisias et al. (2001)
W8709A-13PC	NE Pacific	42.12	−125.75	2712	^{14}C ages	21	Radiolaria, Np Coiling ratios		Pisias et al. (2001); Mix et al. (1999)
ODP 1019	NE Pacific	41.68	−124.93	989	^{14}C ages	63	Radiolaria		Pisias et al. (2001)
ODP 1020	California margin	41.00	−126.43	3038	benthic δ^{18}O	19	$U^{K'}_{37}$		Kreitz et al. (2000)
RC14-105	NW Pacific	39.68	157.55	5630	radiolaria abundance	ca. 3	Radiolaria		Heusser and Morley (1997)
RC14-99	NW Pacific	36.97	147.93	5652	radiolaria abundance	ca. 5	Radiolaria		Heusser and Morley (1997)
KT94-15 PC-9	Japan Sea	39.57	139.41	807	Correlation to KH-79-3 L-3	ca. 13	$U^{K'}_{37}$		Ishiwatari et al. (2001)
GH93 KI-5	Japan Sea	39.57	139.44	754	Correlation to KH-79-3 L-3	ca. 17	$U^{K'}_{37}$		Ishiwatari et al. (2001)
KH-79-3 L-3	Japan Sea	37.06	134.71	935	^{14}C ages, tephra	6.5	$U^{K'}_{37}$		Ishiwatari et al. (1999), (2001)
V1-80-P3	NE Pacific	38.43	−123.80	1600	^{14}C ages on bulk organic C	ca. 10	Radiolaria		Sabin and Pisias (1996)
L13-81-G138	NE Pacific	38.41	−123.97	2531	^{14}C ages on bulk organic C	ca. 8	Radiolaria		Sabin and Pisias (1996)
F8-90-G21	California margin	37.22	−123.24	1605	^{14}C ages	ca. 14	Radiolaria		Sabin and Pisias (1996)
EW9504-13PC	California margin	36.99	−123.27	2510	^{14}C ages	29	Radiolaria		Pisias et al. (2001)
ODP 1018	California margin	36.99	−122.72	2477	benthic δ^{18}O	ca. 36	$U^{K'}_{37}$		Mangelsdorf et al. (2000)
F2-92-P3	California margin	35.62	−121.60	799	^{14}C ages	ca. 22	Radiolaria		Sabin and Pisias (1996)
V1-81-G15	California margin	33.60	−120.42	1000	^{14}C ages	ca. 7	Radiolaria		Sabin and Pisias (1996)
ODP 893	California margin	34.29	−120.04	575	benthic δ^{18}O	170	$U^{K'}_{37}$		Herbert et al. (2001)
EW9504-09PC	California margin	32.86	−119.96	1194	benthic δ^{18}O	10	$U^{K'}_{37}$		Herbert et al. (2001)
ODP 1012	California margin	32.28	−118.38	1772	benthic δ^{18}O	16	$U^{K'}_{37}$		Herbert et al. (2001)
EW9504-03PC	California margin	32.07	−117.37	1245	benthic δ^{18}O	ca. 6	$U^{K'}_{37}$		Herbert et al. (2001)
C-4	Subtropical NW Pacific	33.15	137.70	3343	^{14}C ages	6	Mixed microfossils		Chinzei et al. 1987
KT92-17-St14	Subtropical NW Pacific	32.67	138.46	3252	^{14}C ages	12	$U^{K'}_{37}$		Sawada and Handa (1998)
KT92-17-St19	Subtropical NW Pacific	31.10	138.67	3280	^{14}C ages	14	$U^{K'}_{37}$		Sawada and Handa (1998)
KT92-17-St20	Subtropical NW Pacific	30.38	138.65	3280	^{14}C ages	8	$U^{K'}_{37}$		Sawada and Handa (1998)
V28-304	Subtropical NW Pacific	28.53	134.13	824	benthic δ^{18}O	ca. 5	Radiolaria		Heusser and Morley (1997)
RN95-PC1	East China Sea	32.08	129.00	676	one ^{14}C age, planktonic δ^{18}O	ca. 4	PF		Ujiié and Ujiié (2003)
RN94-PC3	East China Sea	30.93	131.85	1536	^{14}C ages	ca. 13	PF		Ujiié and Ujiié (2003)
RN95-PC3	East China Sea	30.83	128.17	500	^{14}C ages	14	PF		Ujiié and Ujiié (2003)
RN94-PC6	East China Sea	29.75	131.43	3031	one ^{14}C age	ca. 14	PF		Ujiié and Ujiié (2003)
DGKS9603	East China Sea	28.15	127.27	1100	^{14}C ages	13	PF		Li et al. (2001)
RN93-PC3	East China Sea	27.69	126.43	1292	^{14}C ages	ca. 17	PF		Ujiié and Ujiié (2003)
MD982193	East China Sea	27.40	126.27	1614	^{14}C ages	40	PF		Ujiié and Ujiié (2003)
RN93-PC8	East China Sea	24.56	123.75	1561	^{14}C ages	ca. 21	PF		Ujiié and Ujiié (2003)
RN93-PC12	East China Sea	24.02	124.43	2160	^{14}C ages	ca. 9	PF		Ujiié and Ujiié (2003)

RGS0487 BC9/GC11	California margin	23.68	−111.08	381	benthic $\delta^{18}O$	ca. 2	$U^{K'}_{37}$	Herbert et al. (2001)
LPAZ 21P	California margin	22.99	−109.47	624	benthic $\delta^{18}O$	4	$U^{K'}_{37}$	Herbert et al. (2001)
PC20	Subtropical Pacific	21.34	158.17	640	correlated planktic $\delta^{18}O$	2.5	$U^{K'}_{37}$, PF	Lee et al. (2001)
17938-2	South China Sea	19.79	117.54	2840	planktic $\delta^{18}O$	ca. 15	PF	Chen et al. (1999)
17927-2	South China Sea	17.25	119.45	2804	planktic $\delta^{18}O$	ca. 15	PF	Wang et al. (1999)
17954	South China Sea	14.80	111.53	1520	benthic $\delta^{18}O$	6	$U^{K'}_{37}$, PF	Pelejero et al. (1999); Wang et al. (1999)
17961	South China Sea	8.51	112.33	1968	benthic $\delta^{18}O$	11	$U^{K'}_{37}$	Pelejero et al. (1999)
KH92-1-5cBX	W tropical Pacific	3.53	141.87	2282	few ^{14}C ages	ca. 1	$U^{K'}_{37}$	Okhouchi et al. (1994)
ODP 806B	W equatorial Pacific	0.32	159.36	2520	planktic $\delta^{18}O$	4	Mg/Ca	Lea et al. (2000)
W8402A-14GC	Central equat. Pacific	0.95	−138.95	4287	planktic $\delta^{18}O$	ca. 2	$U^{K'}_{37}$	Lyle et al. (1992)
TR163-11	E equatorial Pacific	6.45	−85.82	1950	planktic $\delta^{18}O$	2	PF	Martinez et al. (2003)
ODP677B	E equatorial Pacific	1.20	−83.74	3461	^{14}C age at onset of deglacial	6.5	PF	Martinez et al. (2003)
ODP506B	E equatorial Pacific	0.61	−86.09	2711	^{14}C age in LGM	5	PF	Martinez et al. (2003)
RC13-110	E equatorial Pacific	−0.10	−95.65	3231	benthic $\delta^{18}O$	3	PF	Feldberg and Mix (2003)
TR163-38	E equatorial Pacific	−1.34	−81.58	2200	^{14}C age in LGM	7	PF	Martinez et al. (2003)
TR163-33	E equatorial Pacific	−1.91	−82.57	2230	^{14}C age in LGM	2	PF	Martinez et al. (2003)
ODP846B	E equatorial Pacific	−3.05	−90.49	3307	^{14}C age in LGM	3.5	PF	Martinez et al. (2003)
RR9702A-69TC	Southeastern Pacific	−16.01	−76.33	3228	^{14}C ages, benthic $\delta^{18}O$	5	PF	Feldberg and Mix (2003)
Y71-6-12	Southeastern Pacific	−16.44	−77.56	2734	one ^{14}C age, benthic $\delta^{18}O$	3	PF	Feldberg and Mix (2003)
RR9702A-63TC	Southeastern Pacific	−18.09	−79.04	2901	one ^{14}C age, benthic $\delta^{18}O$	<1	PF	Feldberg and Mix (2003)
TG7	SW Pacific	−17.25	78.11	3120	planktic $\delta^{18}O$	1.5	$U^{K'}_{37}$	Calvo et al. (2001)
P69	SW Pacific	−40.40	178.00	2195	one ^{14}C age, tephra	30	PF	Nelson et al. (2000)
R657	SW Pacific	−42.53	179.49	1408	^{14}C ages	ca. 3	$U^{K'}_{37}$, PF	Sikes et al. (2002)
W268	SW Pacific	−42.85	178.98	980	^{14}C ages	ca. 1	$U^{K'}_{37}$	Sikes et al. (2002)
U939	SW Pacific	−44.53	179.50	1300	^{14}C ages	ca. 6	$U^{K'}_{37}$	Sikes et al. (2002)
U938	SW Pacific	−45.08	179.50	2700	^{14}C ages	ca. 8	$U^{K'}_{37}$, PF	Sikes et al. (2002)
E11-2	Subantarctic S Pacific	−56.00	−115.00	3109	planktic $\delta^{18}O$	9	Mg/Ca	Mashiotta et al. (1999)

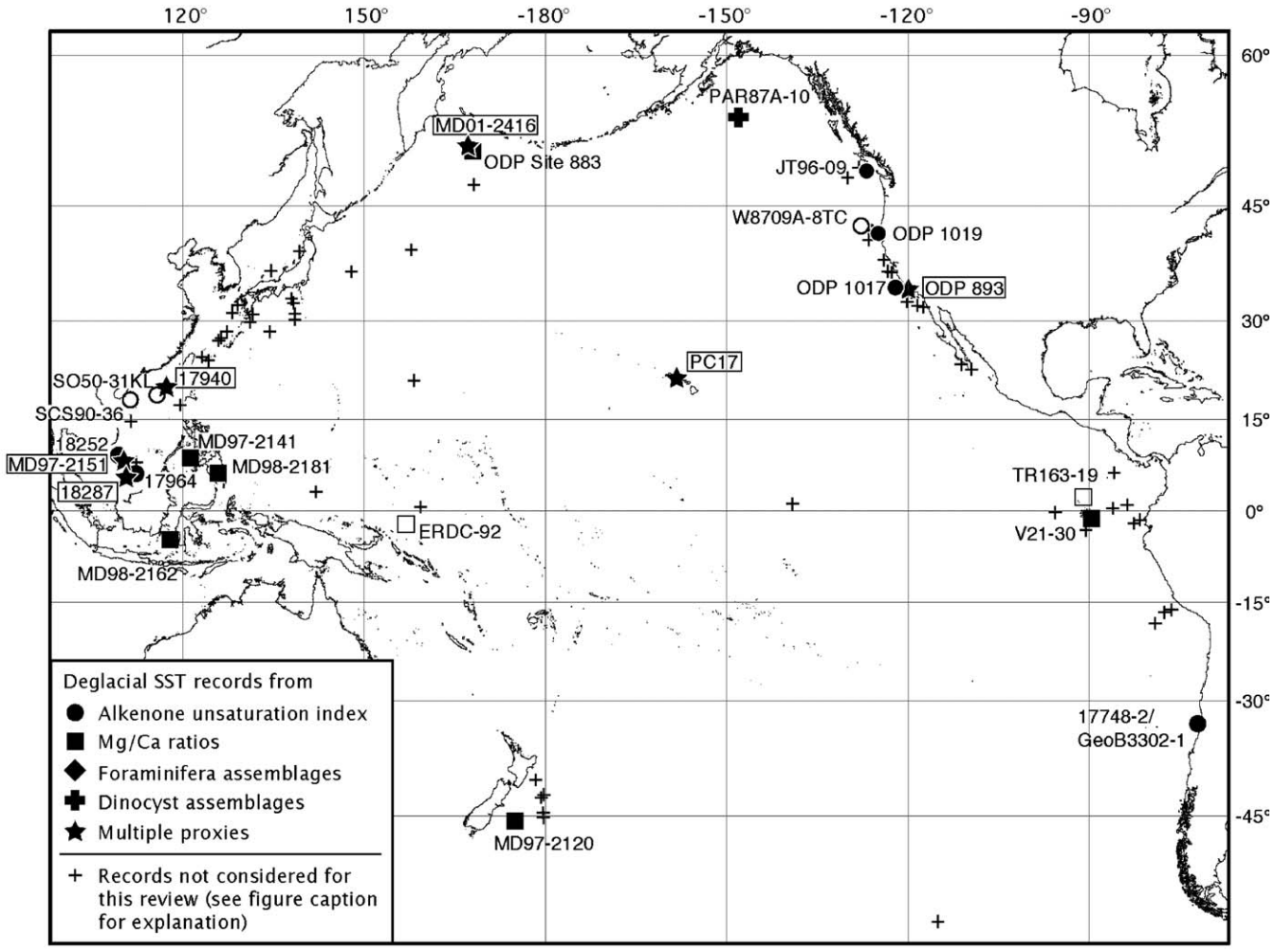

Fig. 1. Distribution of sites with deglacial SST records reviewed in this study (Table 1). Symbols indicate SST estimates derived from alkenones (circles), planktonic foraminiferal Mg/Ca ratios (squares), planktonic foraminiferal assemblages (diamonds), dinocyst assemblages (bold cross) or from multiple proxies (stars with framed core labels, see also Fig. 2). Regional SST patterns (see also Figs. 3–6) are inferred from records with radiocarbon-based age control and high resolution (full symbols), and supported by records with lower resolution (open symbols). Small crosses indicate sites not considered for this review because they lack an independent age control, and/or could not be assigned to a regional SST pattern due to very low resolution or inferred dominance of localized SST variability (see text for discussion).

Grousset et al., 2001), it corresponds to the time of reduced meridional overturning circulation (Sarnthein et al., 1994; McManus et al., 2004) and to the marked deglacial cooling in the North Atlantic region (Cacho et al., 1999; Bard et al., 2000), attributed to the 'Heinrich mode' (Sarnthein et al., 2001; Alley and Clark, 1999) of ocean circulation.

3. Assessment of the multi-proxy approach

Potentials and limitations of comparing different SST proxy records are assessed on the basis of six multi-proxy SST records from different climate regimes of the Pacific, the tropical South China Sea (cores 17940, 18287, and MD97-2151), the central subtropical North Pacific (core PC 17), the eastern mid-latitude Pacific (Santa Barbara Basin, ODP Site 893), and the subarctic northwestern Pacific (core MD01-2416).

The only Pacific site with published SST estimates derived from foraminiferal census counts (Steinke et al., 2001), alkenone unsaturation ($U^{K'}_{37}$; Kienast et al., 2001; Steinke et al., 2001) and foraminiferal Mg/Ca ratios (Whitko et al., 2002) is in the southern South China Sea (site 18287; Fig. 2A). Here, $U^{K'}_{37}$, foraminiferal transfer function (FP-12E) and Mg/Ca estimates consistently record an average late glacial-Holocene SST difference of $2.2 \pm 0.5\,^{\circ}C$. Despite an offset in the absolute SST values, the three methods also agree in recording the main SST features, that is a gradual warming during the later part of H1 (note that this core does not span the entire time interval of H1), an abrupt warming of at least $1\,^{\circ}C$ at ca. 14.7 ka, and a relatively gentle warming towards a mid-Holocene SST maximum (Fig. 2A). An

obvious difference between the three proxy records is the relative smoothness of the alkenone SST record as compared to the more variable foraminiferal Mg/Ca and faunal records (Fig. 2A). This difference could also explain why a minor, albeit clearly detectable, cooling in the $U^{K'}_{37}$-record of 0.2–0.6 °C around 11–13 ka (Steinke et al., 2001) is poorly expressed in the foraminiferal transfer function and Mg/Ca records.

The high-frequency variability of the foraminiferal transfer function and Mg/Ca SSTs could be due to higher sensitivity of the methods, higher analytical noise or higher inherent errors of these approaches. Alternatively, the relatively smooth $U^{K'}_{37}$ record could be due to differential bioturbational mixing of alkenones and foraminifera (Bard, 2001), preferentially attenuating the alkenone record. The excellent agreement (in timing and amplitude) between all methods during the step-like Bølling warming at 14.7 cal ka, however, suggests that this effect is limited to a centimetre-scale. The sample-to-sample agreement, including a synchroneity of foraminiferal $\delta^{18}O$ and $U^{K'}_{37}$ SST, also attests to the autochthonous origin of the alkenones in the South China Sea cores. Whatever the cause(s) for the apparent discrepancy are, the high-frequency variability of foraminiferal transfer function and Mg/Ca SST estimates has the potential to obscure minor SST shifts of less than ~1 °C. For the purpose of this review, however, we note that all three methods of SST estimation clearly show a consistent SST development during the deglaciation.

Similarly, alkenones and a globally calibrated foraminiferal transfer function yield comparable patterns of the deglacial warming at site MD97-2151 in the southwestern South China Sea (Huang et al., 2002), despite differences in the estimated absolute glacial–interglacial SST amplitude (Fig. 2B). In particular, both estimates show a marked cooling during the time interval of H1 (Fig. 2B). Planktonic foraminifera and $U^{K'}_{37}$ also display a comparable deglacial SST development off Hawaii (Lee et al., 2001; see Fig. 2C), thus

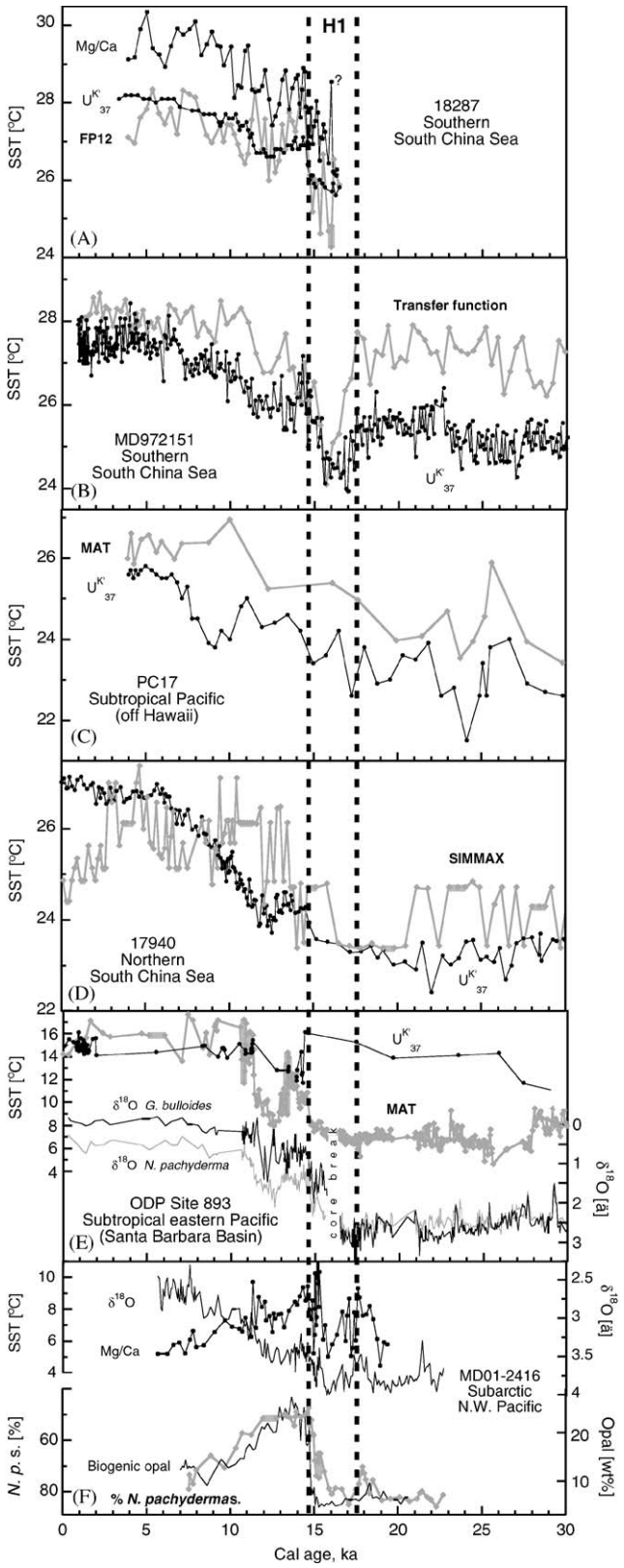

Fig. 2. Multi-proxy SST records from the Pacific (see Fig. 1). A: SST at site 18287 from alkenones, planktonic foraminiferal assemblages using a transfer function (Steinke et al., 2001), and Mg/Ca ratios of *Globigerinoides ruber* (Whitko et al., 2002; calibrated after Lea et al., 2000). (B) SST at site MD97-2151 from alkenones and planktonic foraminiferal assemblages using a foraminiferal transfer function (Huang et al., 2002); (C) SST at site PC17 from alkenones (Lee et al., 2001) and planktonic foraminiferal assemblages using a Modern Analog Technique (MAT; Lee and Slowey, 1999). (D) SST at site 17940 from alkenones (Pelejero et al., 1999) and from planktonic foraminiferal assemblages using the SIMMAX MAT (Pflaumann and Jian, 1999). (E) SST at ODP Site 893 from alkenones (Herbert et al., 2001) and planktonic foraminiferal assemblages using a MAT (Hendy and Kennett, 2000; I. Hendy, unpublished data), compared to $\delta^{18}O$ of *Globigerina bulloides* and *Neogloboquadrina pachyderma* (sinistral + dextral) (Hendy et al., 2002). (F) SST from core MD01-2416 estimated from Mg/Ca ratios of *Neogloboquadrina pachyderma* (sinistral), calibrated after Elderfield and Ganssen (2000), compared to $\delta^{18}O$ of the same species, *N. pachyderma* coiling ratios, and concentrations of biogenic opal (Kiefer et al., submitted).

further justifying the interchangable use of different SST proxies for the purpose of this study.

It is noted, however, that in the South China Sea, various other methods to derive SST estimates from foraminiferal abundances (e.g., SIMMAX, RAM and ANN) yield deviating SST estimates for core MD97-2151 (Chen et al., 2004) and core 18287 (Steinke et al., 2001). Correspondingly, at the northern South China Sea site 17940, a foraminiferal transfer function (SIMMAX) and alkenones yield quite different deglacial SST estimates. For example, an abrupt warming in the $U_{37}^{K'}$ record of ~1 °C at ca 14.7 ka (the Bølling warming) has no equivalent feature in the faunal record, but is instead bracketed by warmings at ~16 and ~13.7 ka (Fig. 2D; Pflaumann and Jian, 1999). Pflaumann and Jian (1999) argue that according to their different habitat the alkenone-producing coccolithophores and planktonic foraminifera record water temperatures from the euphotic zone and the entire upper water column, respectively. However, this deviation between the foraminiferal transfer function and the alkenone unsaturation SST estimates may also be introduced by a large uncertainty of the faunal estimates in the Pacific, arising from a limited number and diversity of coretop samples in the reference datasets (161 samples in Pflaumann and Jian, 1999), which form the basis of this particular SST calibration. This results in frequent poor-analog situations between coretop assemblages and the deglacial assemblages of cores 17940 (and 18287), and in a large sensitivity of the SST estimates to the transfer technique used (see Pflaumann and Jian (1999) and Steinke et al. (2001) for discussion). Thus, in the South China Sea, the discrepancy between different SST estimates appears to be more significant between different foraminiferal transfer techniques (MAT, SIMMAX, RAM, ANN; Steinke et al., 2001 and Chen et al., 2004) than between geochemical proxies (alkenones, Mg/Ca) and Imbrie–Kipp-type foraminferal transfer functions. Since the reason for this inconsistency between the different foraminiferal transfer techniques is not understood yet, we rely on the geochemical SST estimates in assigning a pattern of deglacial SST change in the South China Sea.

It is noted, however, that the timing of changes in the SIMMAX SST record from site 17940, particularly the inferred cold spell between ca. 20 and 16 ka, compares very well to the faunal SST estimates from the Okinawa Trough (Li et al., 2001), possibly indicating a regional signal, at least in foraminiferal abundances. In the Okinawa Trough, however, deglacial SST variability is interpreted to be significantly affected by changes in the geography related to variations in sea level (see the comprehensive review by Ujiié et al., 2003). Furthermore, studies by Brunner and Biscaye (1997) and Yamasaki and Oda (2003) indicate that at shallow water depths foraminiferal tests can be transported laterally, thus potentially obscuring foraminifera-based SST reconstructions at sites of extreme sediment focusing, such as the Okinawa Trough.

In the Santa Barbara Basin alkenones and foraminiferal abundances yield different deglacial SST estimates (Hendy and Kennett, 2000; Herbert et al., 2001). Here, the foraminiferal SST estimates closely follow the planktonic $\delta^{18}O$ records throughout most of the deglaciation, whereas the $U_{37}^{K'}$ SST estimates show a marked cooling of ca 3 °C at the time of the Bølling warm period (Fig. 2E; note, however, that there are no alkenone SST data during the time interval of H1 or the YD). According to Hendy and Kennett (2000), the absolute SST estimates based on the planktonic foraminiferal assemblages in the Santa Barbara Basin are ambiguous due to significant differences (both due to foraminiferal preservation and water column structure) in faunal communities between the Santa Barbara Basin, which is dominated by eurythermal species, and sites in the California Current region and the North Atlantic used to calibrate the transfer methods. Comparing fossil assemblages from the size fraction > 125 μm with calibration data from the standard > 150 μm fraction added further imprecision on the order of ~0.5 °C (Hendy and Kennett, 2000). On the other hand, the alkenone SST estimates may be compromised by the inferred differential preservation of the di- and tri-unsaturated alkenones under oxic and anoxic bottom water conditions (Gong and Hollander, 1999), which would be particularly severe during the abrupt deglacial changes in bottom water oxygenation in the Santa Barbara Basin (Behl and Kennett, 1996). Furthermore, in their regional assessment of alkenone production along the California Margin, Herbert et al. (1998) note that several closely spaced samples from within the Santa Barbara Basin give a considerable range (1.2 °C) of estimated temperatures despite identical modern sea surface temperatures. These authors note, however, that there are significant SST gradients within the basin, which could explain the observed range of surface sediment SST estimates from within the Santa Barbara Basin. It is beyond the scope of this paper to resolve this discrepancy between the faunal and the $U_{37}^{K'}$ SST estimates for the Santa Barbara Basin. Accordingly, we adopt here the interpretation of Hendy et al. (2002) of a close link between the deglacial SST development in the Santa Barbara Basin and Greenland temperatures, which is also substantiated by records of the coiling ratio of *Neogloboquadrina pachyderma* from the same core (Hendy et al., 2002) and Mg/Ca SST estimates from a near-by site (MD02-2504, not shown) in the Santa Barbara Basin (Hill et al., 2003).

Another limitation of SST estimation based on faunal assemblages is revealed by comparing Mg/Ca temperatures and foraminiferal abundances from the subarctic Pacific (site MD01-2416; Fig. 2F; Kiefer et al., submitted). In this case, the foraminiferal census counts

were not converted into SST estimates because no appropriate coretop calibration data set for the subarctic Pacific is currently available. Instead, the relative abundance of the (sub-)polar species *N. pachyderma* (left coiling; *Npl*%) is used as a semi-quantitative SST indicator (see also: Hendy et al., 2002; Elliott et al., 2001). In fact, Mg/Ca and *Npl*%, as well as $\delta^{18}O$ of *N. pachyderma* (left) in core MD01-2416 record the same SST features across the deglacial, which are three warm periods from 18.5 to 16.5 ka, at around 15.5 ka, and from 15–11 ka (Fig. 2F). In detail however, the records fail to agree across the 15–11 ka warm period, when high productivity is suggested by high concentrations of biogenic opal (Fig. 2F). The good (negative) correlation between biogenic opal and *Npl*% suggests that the faunal abundances are modulated by the high productivity conditions (Kiefer et al., submitted), thus cautioning the general use of *Npl*% as an SST indicator. In contrast, the Mg/Ca SST estimates appear to be unaffected by productivity changes and are hence used in this study.

The examples discussed here are certainly insufficient to conclusively rule out minor discrepancies between different SST proxies. In fact, these differences might well contain valuable information regarding variations in seasonality or in the thermal structure of the upper water column. Nevertheless, the records presented here demonstrate that SST estimates from alkenones, foraminiferal Mg/Ca ratios and foraminiferal assemblages generally agree in recording SST changes of more than ~1 °C (see also Bard (2000) for a similar conclusion). Furthermore, it appears that the distinction of different deglacial warming patterns throughout the Pacific (see below) is not affected by the choice of SST proxy.

4. Mapping common SST patterns

Bearing in mind the uncertainties related to the multi-proxy approach, we review in the following section the SST development during the deglaciation in currently available downcore records from the Pacific Ocean, focussing on the time interval of H1.

4.1. Continuous deglacial warming

The SST records compiled in Fig. 3 show a continuous deglacial warming, starting at around 19 ± 1 ka, which corresponds to the end of the Last Glacial Maximum (as defined by Mix et al., 2001). All these records have in common that there is no clear indication of a cessation of the deglacial SST increase during H1 (or the ACR or the YD), and that roughly half the deglacial warming occurs prior to the end of H1, i.e. prior to the onset of the Bølling warming. This pattern of continuous deglacial warming is characteristic of the tropical and subtropical open Pacific (Figs. 3B–F), including the Sulu Sea (Fig. 3E), as well as of the Peru-Chile current off mid-latitude Chile (Fig. 3G) and possibly of the southeastern subantarctic Pacific (site E11-2; Mashiotta et al., 1999; not shown).

It is conceivable that the continuous warming trend observed in some of the lower resolution records or in records from lower sedimentation rate sites is merely due to unresolved SST variations or bioturbational attenuation of the signal, respectively. For example, two $U^{K'}_{37}$ SST records from sites in the South China Sea with low sedimentation rates (average 6–10 cm/kyr, Table 1) show only reduced deglacial SST oscillations characteristic of this marginal basin (see below). Instead, these records display a more or less continuous deglacial warming (Huang et al., 1997a,b; not shown). However, a number of sites from this group, particularly in the western equatorial Pacific, clearly have high enough resolution and sedimentation rates (Table 1) to resolve millennial-scale events such as H1, the ACR or the YD. The lack of any SST response during H1 suggests that the deglacial warming of this region was not affected by changes in the intensity of the MOC, and/or in the atmospheric circulation associated with H1. Furthermore, accepting that the first step in sea level rise occurred at ca 19 ka (see Lambeck and Chappell (2001) for review), the onset of the warming appears to be in phase with the initial melting of continental ice sheets.

4.2. The Antarctic type deglacial pattern

The Antarctic type SST pattern is similar to the continuous deglacial warming described above (i.e., temperatures increased gradually across H1), but punctuated by a moderate temperature decrease during the Allerød period, coeval with the ACR found in Antarctic ice cores (around 13–14 ka; Blunier et al. 1997). Because of the brevity of the ACR (~1000 years) and its relative low-amplitude signal it is difficult to unambiguously distinguish the Antarctic-type deglacial warming from the continuous warming pattern described above. Nevertheless, we adopt here the interpretation of Pahnke et al. (2003) of the deglacial Mg/Ca SST record of core MD97-2120 off New Zealand as showing an ACR (Fig. 3(H)). In contrast to this record, neither of the tropical or subtropical and subantarctic SE Pacific records show any clear indication of an ACR. However, as discussed above, this lack of an ACR signal could also be due to signal attenuation due to low sedimentation rates, most notably in the only other record from the subantarctic Pacific (site E11-2; Mashiotta et al., 1999) or due to low sampling frequency (e.g. site P69 off New Zealand; Nelson et al., 2000). Accordingly, the extent of the Antarctic-type signal cannot be mapped properly. However, the few SST records available suggest that, contrary to the Atlantic

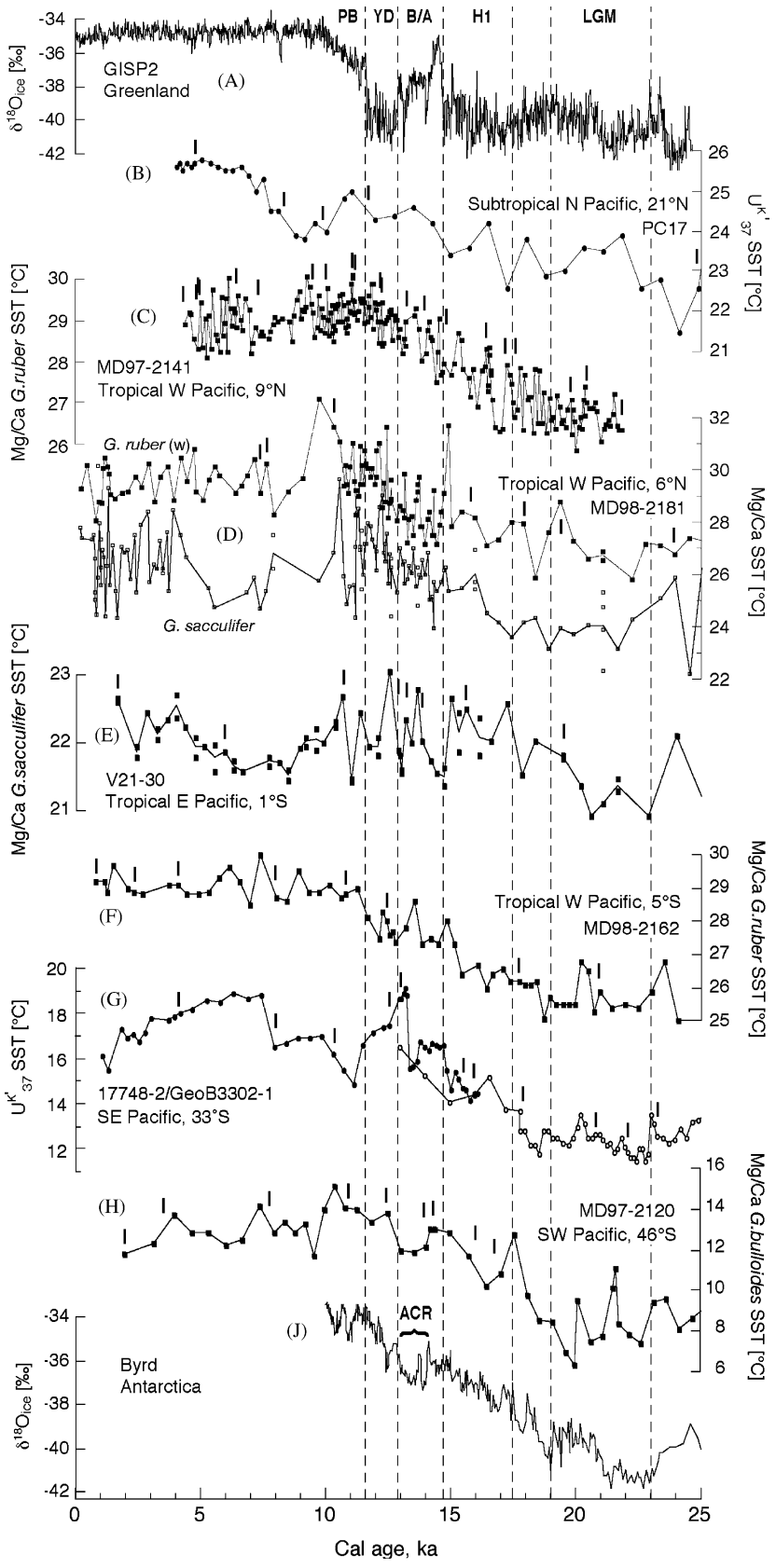
PB
YD
B/A
H1
LGM
GISP2
Greenland
(A)
δ18Oice [‰]
(B)
Subtropical N Pacific, 21°N
PC17
UK'37 SST [°C]
(C)
MD97-2141
Tropical W Pacific, 9°N
Mg/Ca G.ruber SST [°C]
G. ruber (w)
(D)
Tropical W Pacific, 6°N
MD98-2181
G. sacculifer
Mg/Ca SST [°C]
(E)
V21-30
Tropical E Pacific, 1°S
Mg/Ca G.sacculifer SST [°C]
(F)
Tropical W Pacific, 5°S
MD98-2162
Mg/Ca G.ruber SST [°C]
(G)
17748-2/GeoB3302-1
SE Pacific, 33°S
UK'37 SST [°C]
(H)
MD97-2120
SW Pacific, 46°S
Mg/Ca G.bulloides SST [°C]
ACR
(J)
Byrd
Antarctica
δ18Oice [‰]
Cal age, ka

(e.g. Rühlemann et al., 1999), a link between SSTs and air temperatures over Antarctica is restricted to the region of circum-Antarctic atmospheric circulation. It is noted, however, that based on planktonic foraminiferal $\delta^{18}O$ records from the Pacific sector of the Southern Ocean and from the Great Australian Bight, respectively, Morigi et al. (2003) and Andres et al. (2003) postulate the occurrence of a cooling event coeval with the YD cold period in the Southern Ocean. If corroborated by independent SST estimates, these findings challenge the interpretation of Pahnke et al. (2003) of a close coupling of the South Pacific to Antarctic climate variability during the deglaciation.

4.3. Warm-cold oscillation during H1

Two SST records from the subarctic northwestern Pacific (sites ODP 883 and MD01-2416) and one record from the California margin (ODP Site 1017E) are characterized by a rapid warming leading into an SST maximum during the older part of H1 (ca. 18.5–16.5 ka), followed by a cooling during the younger part of H1 (ca. 16.5–15.5 ka) and another rapid warming towards the end of H1 (ca 15.2 ka; Fig. 4C, D, G). Whether or not the abrupt warming following this cold spell could be synchronous with the Bølling warming in the circum-North Atlantic realm will be discussed below. A similar pattern, albeit with lower resolution, is also evident in the SST record based on dinocyst assemblages from the subarctic northeastern Pacific (Fig. 4B). The only two other high-resolution SST records published from the North Pacific to date (sites JT96-09 and ODP 1019; Fig. 4E, F) do not cover the period of interest here. Nevertheless, it is noteworthy that both these $U^{K'}_{37}$ SST records show a warm spike preceding the inferred Bølling warming, possibly indicating that the warm-cold oscillation described above is characteristic of the entire North Pacific. On the other hand, both these records show a YD-type cooling, supporting a close coupling to North Atlantic climate variability during this climate event.

The abrupt warming at the termination of the late-H1 cold spell occurs at ca 15.5 ka at sites ODP 883 and MD01-2416 as well as at site ODP 1017. In core MD01-2416, the age of this warming is constrained by numerous, closely spaced AMS ^{14}C dates, which allow identification in the sediment core of the ^{14}C plateau occurring from ca 12.4–12.7 ^{14}C ka (ca 15.3–14.35 cal. ka; Stuiver et al., 1998; Hughen et al., 2004). Thus, the dates of 12,460 ^{14}C years (reservoir-corrected) near the top and 12,470 ^{14}C years near the base of the radiocarbon plateau identified in the NW Pacific core MD01-2416 provide crucial age control points with centennial precision around 14.35 and 15.3 ka (Fig. 4C; Kiefer et al., submitted; Sarnthein et al., 2003). The fact that the ^{14}C dates defining the plateau occurs significantly after the SST maximum constitutes compelling evidence that the warming in the NW Pacific occurred several hundred years before the Bølling warming in Greenland at 14.7 cal. ka (Kiefer et al., submitted). This approach of using known features of the ^{14}C curve to establish age fixpoints is analogous to a recent study by Hajdas et al. (2003), who used the Younger Dryas radiocarbon plateau to constrain the timing of cold events in South America.

At ODP Site 1017A off California, the warming at 15.5 ka is delimited by three radiocarbon dates (see Fig. 4). The ^{14}C age closest to the abrupt SST increase (13,050 years at 300.5 cm corrected depth) yields two calibrated ages according to CALIB 4.3 (using a local reservoir age anomaly ΔR of 233 years; Kennett et al., 2000) of 14.37–14.14 and 15.17–14.64 ka (both 1σ), respectively. Choosing the former intercept places the midpoint of the abrupt warming at ca. 14.8 ka, which is indistinguishable from the age of the Bølling warming in the GISP2 ice core record. However, choosing the older intercept produces an age of ca. 15.3 ka, suggesting a lead of this warming with respect to the Bølling warming in the North Atlantic. Omitting this ^{14}C date from the age model (as per Kennett et al., 2000, and adopted by Seki et al., 2002), and interpolating between the two immediately adjacent ^{14}C dates (which have low 1σ calendar age ranges) corroborates the older age of the abrupt warming (Fig. 4G). Even though there does not seem to be any a priori reason to cull the age at 300.5 cm, assuming more or less constant sedimentation rates at this site, would further corroborate the older age of $\sim$15.5 ka of this event.

The temperature fluctuation during H1 described here represents a departure from the simple antiphasing of the northeastern Pacific with respect to North Atlantic climate variability postulated to occur during Dansgaard–Oeschger events (Kiefer et al., 2001), and precludes a direct response of North Pacific SSTs to a

Fig. 3. SST records characterized by a continuous warming across the deglacial without major intermittent coolings, compared to the $\delta^{18}O$ records from ice cores in Greenland (A; GISP2; Stuiver and Grootes, 2000) and Antarctica (J; Byrd; Blunier et al., 1998). SST records are arranged North-South: (B) PC17 (Lee et al., 2001), (C) MD97-2141 (Rosenthal et al., 2003), (D) MD98-2181 on a recalculated age scale by linearly interpolating between calibrated ^{14}C ages; lines connect averages of multiple SST data (Stott et al., 2003), (E) V21-30 (Koutavas et al., 2003), (F) MD98-2162 (Visser et al., 2003), (G) 17748-2 and GeoB3302-1 (Kim et al., 2002), (H) MD97-2120 (Pahnke et al., 2003). The latter record shows a 1–2 °C ACR-type cooling during the Allerød. Dashes above SST records mark ^{14}C dates used for the age models, adopted from the original publications. PB = Preboreal, YD = Younger Dryas, B/A = Bølling/Allerød, H1 = Heinrich event 1, LGM = Last Glacial Maximum, ACR = Antarctic Cold Reversal. Symbols as in Fig. 1.

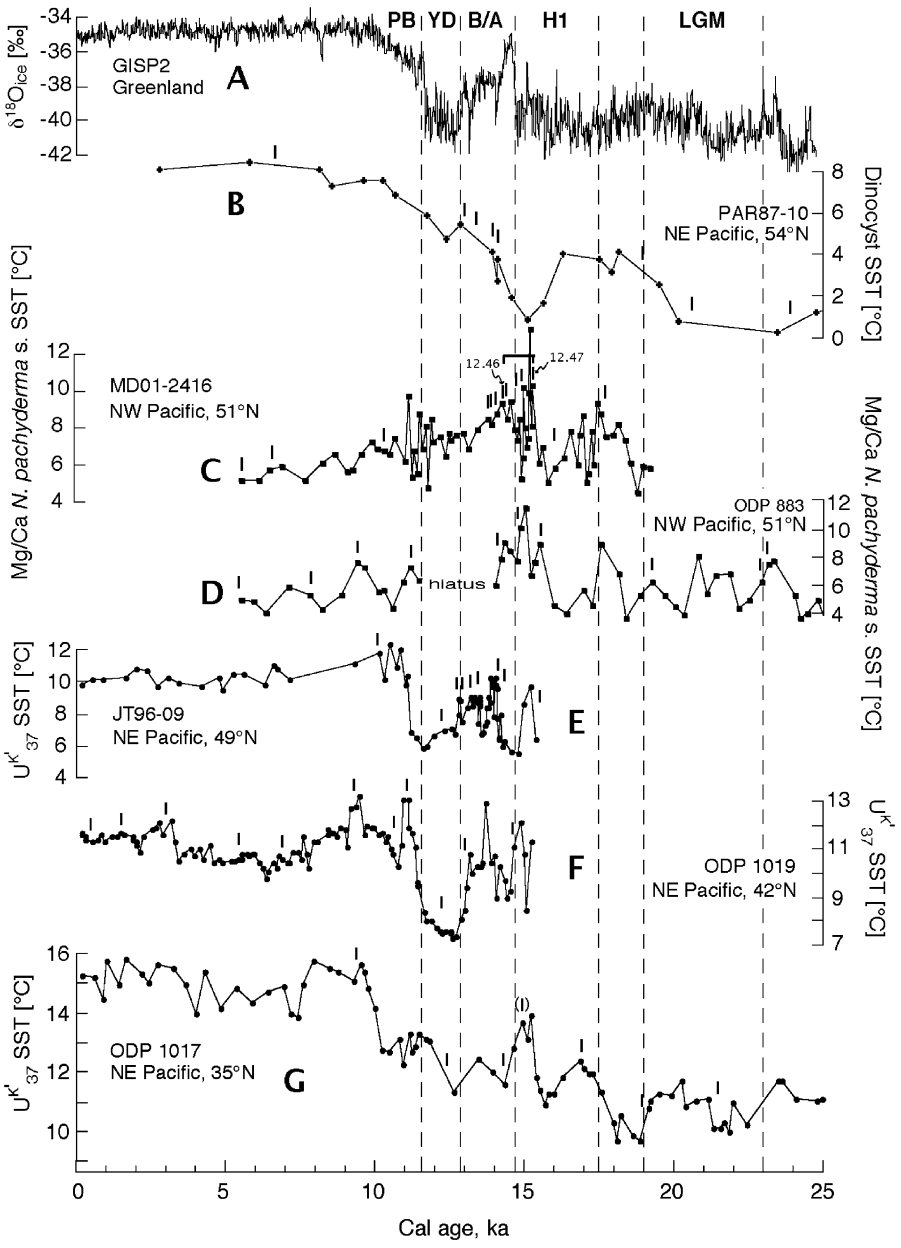

Fig. 4. SST records across the deglacial showing a warm-cold oscillation during H1 compared to the $\delta^{18}O$ record from Greenland ice core GISP2 (A; Stuiver and Grootes, 2000). SST records are arranged North-South: (B) PAR87-10 (de Vernal and Pedersen, 1997) on a recalibrated time scale, (C) MD01-2416 (Kiefer et al., submitted) with horizontal bar delineating the ^{14}C-Plateau at 12.4-12.7 ^{14}C ka used as a time marker for late H1/early Bølling (see text), (D) ODP Site 883 (Kiefer et al., submitted), (E) JT96-09 (Kienast and McKay, 2001), (F) ODP Site 1019 (Barron et al., 2003) on their untuned age scale, and (G) ODP Site 1017 (Seki et al., 2002). Dashes and abbreviations as in Fig. 3. The dash in brackets at ODP Site 1017 marks the position of the culled ^{14}C age discussed in the text. Numbers at MD01-2416 give the reservoir corrected ^{14}C ages defining the extent of the 14C plateau (see text). Symbols as in Fig. 1.

shut down of the MOC during H1. Even though the old age of the termination of this inter-H1 cold spell at ca. 15.5 ka is less than 800 years older than the GISP2 age of the Bølling warming (i.e., within the potential error of ^{14}C chronologies), we still suggest that it is a true feature because it is evident in three independent records, constrained by numerous AMS ^{14}C dates. Furthermore, we note that an analogous 'pre-Bølling warming' event is also seen in records of *N. pachyderma* coiling ratios off Oregon and northern California (sites ODP 1019 and W8709A-13PC; Mix et al., 1999), and in the Santa Barbara Basin (Hendy et al., 2002). This observation also demonstrates the critical role of high resolution age control for revealing offsets in timing and duration of climate events, which otherwise might have been assumed to occur synchronously.

Due to the limited number of northern Pacific SST records, the mapping of the regional extent of this pattern is vague, in particular in the western and central Pacific. Differing SST patterns in the East China and South China Seas and near Hawaii define a maximum southern limit. At the east Pacific margin the southernmost site clearly reflecting the H1 warm-cold oscillation is ODP Site 1017 at 34.5°N. Thus, records of the warm-cold oscillation are currently restricted to the northern subarctic gyre and its southward extension, the California Current. This could be taken as an indication that the SST signal 'originates' somewhere in the subarctic Pacific and is then transmitted further across the North Pacific, possibly by surface currents.

4.4. The marginal sea type

The SST records of the marginal basins of the Pacific (South China Sea, Santa Barbara Basin) show a rapid warming synchronous (within the errors of radiocarbon chronology) with the Bølling warming in GISP2 (Fig. 5). This abrupt rise in SST is preceded by a SST minimum or a period of reduced warming during the time of H1. Both the low SSTs during H1 as well as the following rapid warming at ca. 14.7 ka are analogous to the GISP2 pattern (Fig. 5A) and suggest a strong coupling to the deglacial climate development of the North Atlantic region. This interpretation of the SST pattern in the South China Sea is not only corroborated by five independent $U^{K'}_{37}$ SST records from throughout the South China Sea that all show an abrupt warming at ca. 14.7 ka (Pelejero et al. 1999, Wang et al., 1999; Kienast et al., 2001; see Kienast et al., 2003, and Sarnthein et al., 2003, for a discussion of the ^{14}C dates of Wang et al. 1999; Huang et al., 2002) but also by the general agreement of multiple proxies (Steinke et al. 2001; Huang et al., 2002; Figs. 2A, B).

The interpretation of the Santa Barbara Basin record is more complicated. First, the interpretation of this record with respect to SST during H1 is compromised by a core break during part of the time interval of H1 (ca. 16.6–15.7 ka; Fig. 5B). Secondly, there is a significant discrepancy between the different deglacial SST estimates depending on the proxy used (see above). Nevertheless, the good agreement between foraminiferal abundance (Hendy and Kennett, 2000) and Mg/Ca (Hill et al., 2003) SST estimates suggests a close link of temperatures in this basin to the deglacial warming in Greenland. Some of the marine records described here do not show an actual cooling during H1 as evident in Greenland ice cores and North Atlantic sediment records but rather a slow rate of warming (Figs. 5B, C). Thus, we interpret these records as a combination of the North Atlantic type deglaciation and the continuous warming trend described above for the open low-latitude Pacific. Given the fact that both the Santa Barbara Basin and particularly the South China Sea are surrounded by open ocean records that show very different patterns (see above), the most likely communication of these marginal basins and the North Atlantic is through the atmosphere (sensu Mikolajewicz et al., 1997).

The assertion of a deglacial SST pattern typical of marginal seas is further substantiated by an analogous discrepancy between the deglacial SST increase in the Cariaco Basin (Lea et al., 2003) compared to the open western tropical Atlantic (Rühlemann et al., 1999) and the Gulf of Mexico (Flower et al., 2004). Thus, the Cariaco Basin SST record shows a Greenland-type SST increase at the onset of the Bølling period, whereas the western tropical Atlantic and the Gulf of Mexico show a close coupling to Antarctic temperatures during the deglaciation, in line with the bipolar see-saw mechanism. Taken together, these records suggest that SSTs in marginal seas are influenced more significantly by continental/atmospheric variability than open ocean sites.

5. Discussion and conclusions

As more records become available, the generalized classification of the deglacial warming in the Pacific proposed here (Fig. 6) may be replaced by the realization of a regionally even more diverse and spatially more dynamic deglacial warming throughout the Pacific. Examples of this highly localized variability are available already from the Japan Sea, the East China Sea and the Kuroshio region, where sea level-related changes in the geographic and oceanographic setting and minor changes in the flow path of the Kuroshio warm current, respectively, have been shown to have profound effects on the deglacial warming on a very localized spatial scale (Sawada and Handa, 1998; Ishiwatari, 1999, 2001; Kim et al., 2000; Ujiié et al., 2003). Similarly, recent studies by Martinez et al. (2003), Koutavas and Lynch-Stieglitz (2003), and Feldberg and Mix (2003) demonstrate a high degree of complexity and regionality in the eastern equatorial Pacific. Here, SSTs are affected by the interaction of equatorial upwelling dynamics, including potential changes in the temperature of the source waters, with changes in the meridional SST gradients related to the intensity and position of the Intertropical Convergence Zone (ITCZ), and variable advection of water masses from the Peru Current. Finally, the northeast Pacific off California and Oregon is another example of high spatial heterogeneity during the deglaciation. Here, SSTs are postulated to be driven by an interaction of the intensity of the California Current and Countercurrent, extent of the North Pacific gyre, and the intensity and position of coastal and open ocean upwelling (Mix et al., 1999; Herbert et al., 2001;

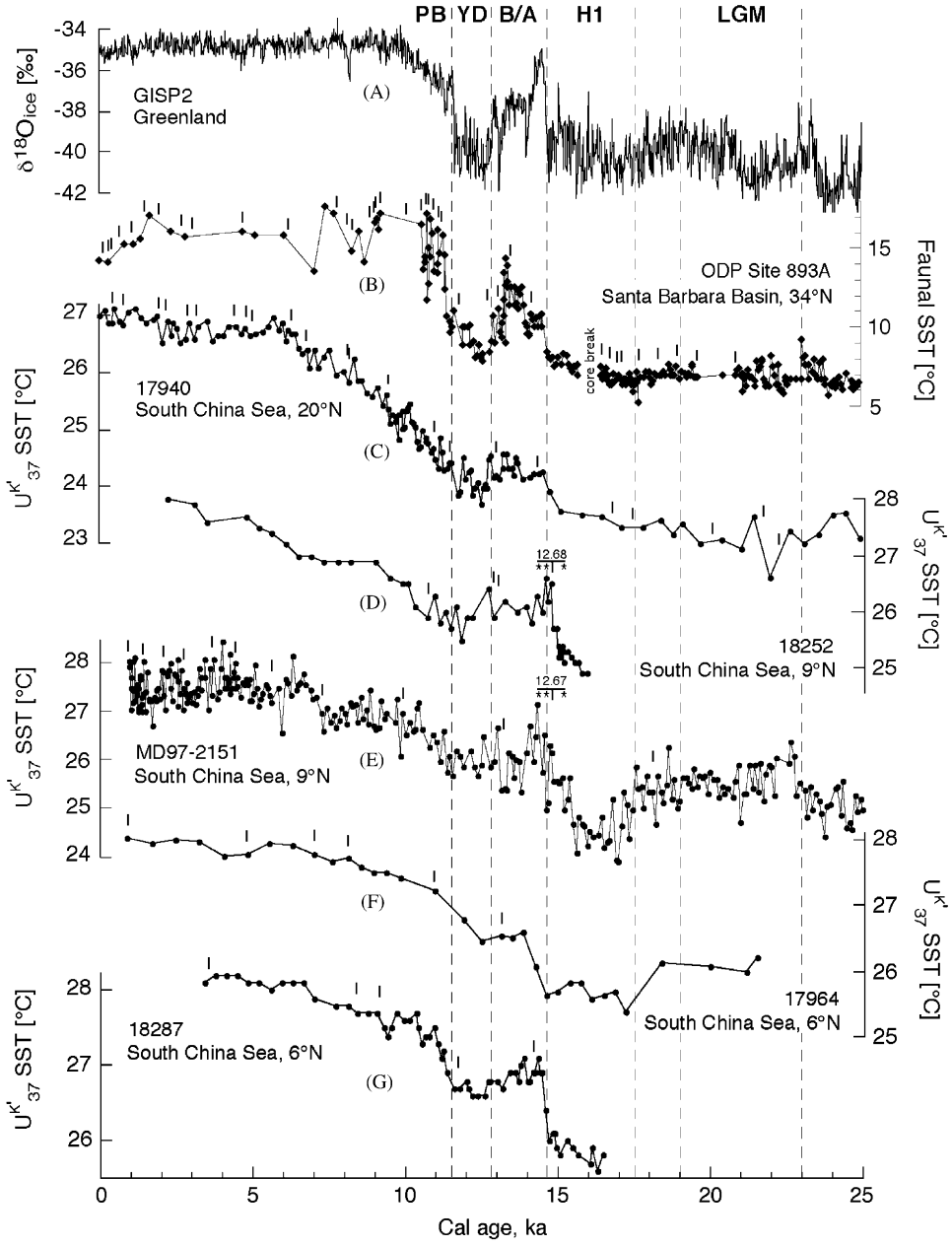

Fig. 5. SST records with 'Greenland-type' deglacial pattern compared to the $\delta^{18}O$ record from Greenland ice core GISP2 (A; Stuiver and Grootes, 2000). SST records are arranged North-South: (B) ODP Site 893 (Hendy and Kennett, 2000; I. Hendy, unpublished SST estimates from planktonic foraminiferal assemblages; Hendy et al., 2002)), (C) 17940 (Pelejero et al., 1999), (D) 18252 (Kienast et al., 2001), (E) MD97-2151 (Huang et al., 2002) on a recalibrated age scale after Lee et al. (1999), (F) 17964 (Pelejero et al., 1999), (F) 18287 (Steinke et al., 2001). Dashes and abbreviations as in Fig. 3. Symbols as in Fig. 1. Asterisks in D and E mark the three alternative intercept ages of the respective ^{14}C dates with the calibration curve of Stuiver et al. (1998), the average age of which (dash in between) was used for the age models.

Pisias et al., 2001; Hendy et al., 2002). In both of these cases, however, some of the inferred regionality of the deglacial warming could also be related to subtle discrepancies between the diverse proxies used to reconstruct SSTs at different sites within the same region (i.e., foraminiferal and radiolarian transfer functions, N. *pachyderma* coiling ratios, alkenones, foraminiferal Mg/Ca and planktonic foraminiferal $\delta^{18}O$).

It appears, however, that even the limited number of SST records available to date allows some key conclusions to be drawn about the deglacial warming in the Pacific:

(1) A close coupling of the deglacial SST increase in the Pacific to temperatures in the North Atlantic realm appears to be restricted to the marginal seas (Fig. 6), possibly also including some marginal sites along the northeastern Pacific. This calls for an at least northern

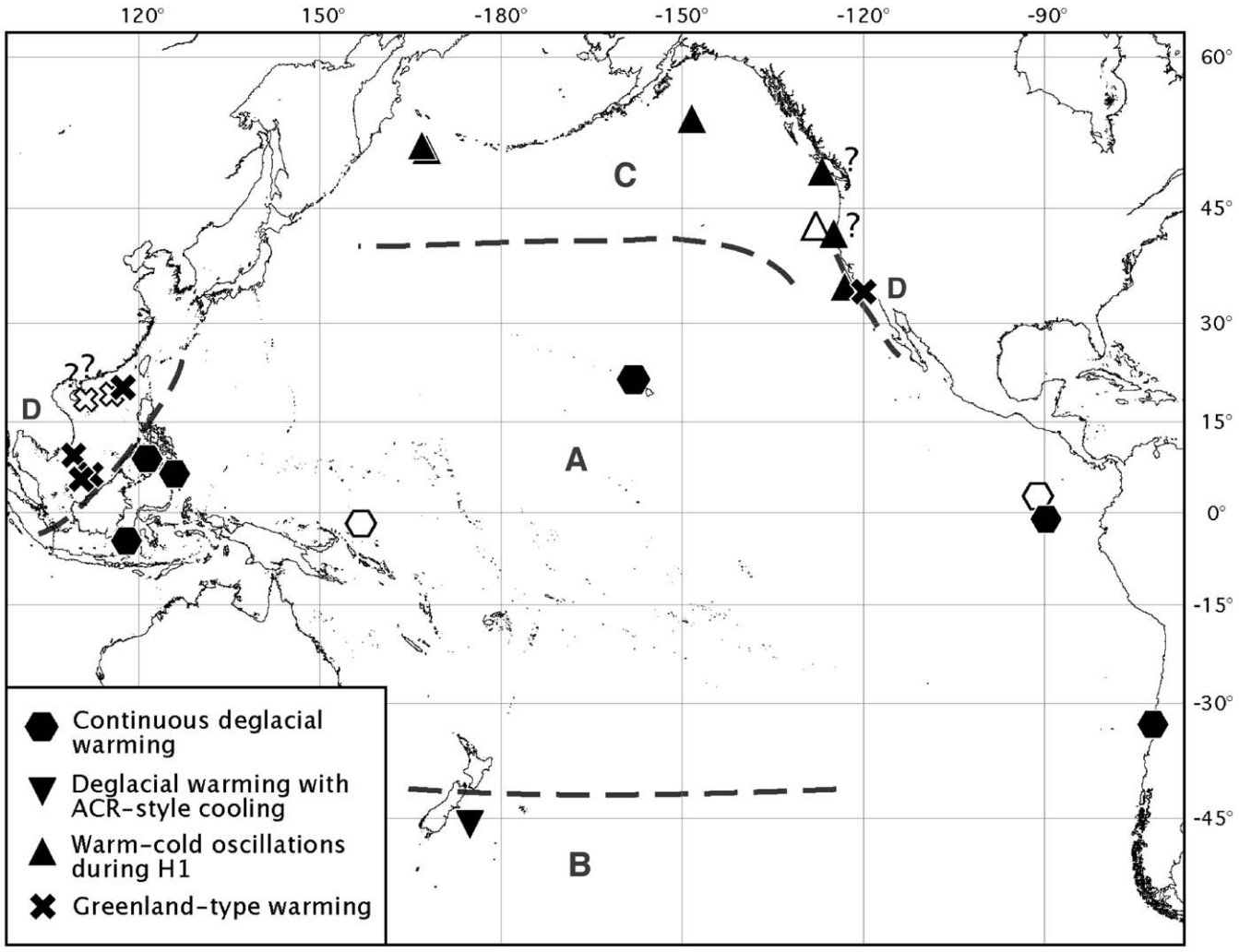

Fig. 6. Distribution of the four endmember-type deglacial SST patterns (A–D) in the Pacific: Continuous deglacial warming (hexagons, "A", Fig. 3B–G), deglacial warming with Antarctic Cold Reversal-style cooling (inverse triangle, "B", Fig. 3(H), warm-cold oscillations during Heinrich event 1 (triangles, "C", Fig. 4), and stepwise Greenland-type warming (crosses, "D", Fig. 5). Full and open symbols as in Fig. 1. The dashed grey lines outline the presumed regional extent of patterns A–D.

hemisphere-wide atmospheric teleconnection (sensu Mikolajewicz et al., 1997), which appears to be overwhelmed by different, and yet unexplained, processes governing the deglacial rise in SSTs in the more open oceanic settings.

(2) To the extent that the records presented here are representative of regional-scale deglacial warming patterns, there does not seem to be any obvious and/or dominant response of open ocean SSTs in the Pacific to the H1 reduction of the MOC or the associated cooling in the North Atlantic. This challenges some of the mechanisms that have been proposed to influence glacial-interglacial SST variability, particularly in the equatorial Pacific. For example, the persistent and pronounced cooling in the North Atlantic such as during H1 would increase the meridional gradients of SST and surface air temperature, resulting in intensified trade winds and a south-ward migration of the ITCZ (Schiller et al., 1997). Both these atmospheric effects have been invoked to explain glacial-interglacial changes in SST along the equatorial upwelling zone, and in the eastern equatorial Pacific, respectively, and should thus lead to SST variations associated with H1 in this region as well. We concede, however, that the resolution and sensitivity of the presently available SST records from the eastern equatorial Pacific might not suffice to record any subtle SST variations linked to H1. Furthermore, a recent model study by Chiang et al. (2003) suggests that any displacement of the ITCZ due to changes in the intensity of the MOC could be offset by an opposing effect of North Atlantic sea ice cover on the position of the ITCZ. Finally, the inferred absence of an SST response during H1, particularly in the low latitude Pacific (Figs. 3 and 6), is generally consistent with many

climate models that show only very minor changes in the tropical Pacific in response to a collapse of the MOC (e.g., Vellinga and Wood, 2002; Schmittner et al., 2003).

(3) The warm-cold oscillations in the northern North Pacific (Figs. 4 and 6) reveal a high degree of centennial-scale climate variability within the time interval of H1. For the North Atlantic region, a comparable variability within the time interval of H1 has been proposed to account for the variable origin and abundance of icebergs (Bond and Lotti, 1995; Elliot et al., 1998; Bard et al., 2000; Grousset et al., 2001), and for the fluctuating intensity of atmospheric polar circulation (Rohling et al., 2003). Nevertheless, regional temperatures remained invariably cold throughout H1 in the North Atlantic region (Bond et al., 1993; Bard et al., 2000; Stuiver and Grootes, 2000), indicating a high sensitivity of northern Pacific SSTs to yet unspecified climate perturbations during H1. Most notably, the internal SST variability during H1 in the subarctic northwest Pacific is decoupled from records of marine productivity from the same cores (Kiefer et al., submitted), suggesting that it is not primarily driven by changes in water column stratification and/or upwelling of sub-surface waters.

(4) The contrasting patterns of deglacial warming observed in various parts of the Pacific (Fig. 6) imply that both zonal and meridional gradients changed on centennial (or even shorter) timescales during the deglaciation. This will complicate any 'simple' reconstruction of meridional and/or zonal temperature gradients, as well as of inferred water vapour fluxes between the Pacific and Atlantic Oceans.

(5) The radiocarbon-dated SST records from the tropical and subtropical Pacific constrain the deglacial warming to have started at $19+/-1$ ka BP. Thus, the warming appears to be in phase with the initial melting of continental ice sheets.

Acknowledgements

This work was made possible through the generous sharing of data and manuscripts by a large number of colleagues. In particular we thank Ingrid Hendy for making available to us her unpublished faunal SST data of ODP Site 893. S. Kienast and T. F. Pedersen kindly provided a revised age model for core PAR87-10. The study benefited from discussions with and comments by S. Kienast, D. Lea, O. Marchal, D. Oppo, C. Pelejero, and M. Sarnthein. We owe our thanks to all MARGO participants for inspiration and exchange of data and ideas. The manuscript benefited from constructive reviews by P. Clark and an anonymous reviewer. Funding through the UK Natural Environmental Research Council (NER/A/S/2000/00493; TK) and a WHOI postdoctoral scholarship (Devonshire Foundation; MK) is gratefully acknowledged. This is WHOI contribution 10994.

References

Alley, R.B., Clark, U., 1999. The deglaciation of the northern hemisphere: a global perspective. Annual Review of Earth and Planetary Science 27, 149–182.

Alley, R.B., Brook, E.J., Anandakrishnan, S., 2002. A northern lead in the orbital band: north–south phasing of Ice-Age events. Quaternary Science Reviews 21, 431–441.

Andres, M.S., Bernasconi, S.M., McKenzie, J.A., Röhl, U., 2003. Southern Ocean deglacial record supports global Younger Dryas. Earth and Planetary Science Letters 216, 515–524.

Bard, E., 2000. Comparison of alkenone estimates with other temperature proxies. Geochemistry Geophysics Geosystems 2, 1–12.

Bard, E., Rostek, F., Turon, J.-L., Gendreau, S., 2000. Hydrological impact of Heinrich Events in the subtropical northeast Atlantic. Science 289, 1321–1324.

Bard, E., 2001. Paleoceanographic implications of the difference in deep-sea sediment mixing between large and fine particles. Paleoceanography 16, 235–239.

Barron, J.A., Heusser, L., Herbert, T., Lyle, M., 2003. High-resolution climatic evolution of coastal northern California during the past 16,000 years. Paleoceanography 18 10.1029/2002PA000768.

Behl, R.J., Kennett, J.P., 1996. Brief interstadial events in the Santa Barbara basin, NE Pacific, during the past 60 kyr. Nature 379, 243–246.

Blunier, T., Schwander, J., Stauffer, B., Stocker, T., Dällenbach, A., Indemühle, A., Tschumi, J., Chappellaz, J., Raynaud, D., Barnola, J.-M., 1997. Timing of the Antarctic Cold Reversal and the atmospheric CO_2 increase with respect to the Younger Dryas event. Geophysical Research Letters 24, 2683–2686.

Blunier, T., Chappellaz, J., Schwander, J., Dällenbach, A., Stauffer, B., Stocker, T.F., Raynaud, D., Jouzel, J., Clausen, H.B., Hammer, C.U., Johnsen, S.J., 1998. Asynchrony of Antarctic and Greenland climate change during the last glacial period. Nature 394, 739–743.

Brunner, C.A., Biscaye, P.E., 1997. Storm-driven transport of foraminifers from the shelf to the upper slope, southern Middle Atlantic Bight. Continental Shelf Research 17, 491–508.

Bond, G., Heinrich, H., Broecker, W., Labeyrie, L., McManus, J., Andrews, J., Huon, S., Jantschik, R., Clasen, S., Simet, C., Tedesco, K., Klas, M., Bonani, G., Ivy, S., 1992. Evidence for massive discharges of icebergs into the North Atlantic ocean during the last glacial period. Nature 360, 245–249.

Bond, G., Broecker, W., Johnsen, S., McManus, J., Labeyrie, L., Jouzel, J., Bonani, G., 1993. Correlations between climate records from North Atlantic sediments and Greenland ice. Nature 365, 143–147.

Bond, G.C., Lotti, R., 1995. Iceberg discharges into the North Atlantic on millennial time scales during the last glaciation. Science 267, 1005–1010.

Broecker, W.S., 1998. Paleocean circulation during the last deglaciation: a bipolar seesaw? Paleoceanography 13, 119–121.

Broecker, W.S., Hemming, S., 2001. Climate swings come into focus. Science 294, 2308–2309.

Cacho, I., Grimalt, J.O., Pelejero, C., Canals, M., Sierro, F.J., Flores, J.A., Shackleton, N., 1999. Dansgaard-Oeschger and Heinrich event imprints in Alboran Sea paleotemperatures. Paleoceanography 14, 698–705.

Calvo, E., Pelejero, C., Herguera, J.C., Palanques, A., Grimalt, J.O., 2001. Insolation independence of the southeastern Subtropical

Pacific sea surface temperature over the last 400 kyrs. Geophysical Research Letters 28, 2481–2484.

Chen, M.-T., Wang, C.-H., Huang, C.-Y., Wang, P., Wang, L., Sarnthein, M., 1999. A late Quaternary planktonic foraminifer faunal record of rapid climatic changes from the South China Sea. Marine Geology 156, 85–108.

Chen, M.-T., Huang, C.-C., Pflaumann, U., Waelbroeck, C., Kucera, M., 2005. Estimating glacial western Pacific sea-surface temperature: methodological overview and data compilation of surface sediment planktic foraminifer faunas. Quaternary Science Reviews this issue.

Chiang, J.C.H., Biasutti, M., Battisti, D.S., 2003. Sensitivity of the Atlantic Intertropical Convergence Zone to Last Glacial Maximum boundary conditions. Paleoceanography 18 10.1029/2003PA000916.

Chinzei, K., Fujioka, K., Kitazato, I., Koizumi, I., Oba, T., Oda, M., Okada, H., Sakai, T., Tanimura, Y., 1987. Postglacial environmental changes of the Pacific Ocean off the coasts of central Japan. Marine Micropaleontology 11, 273–291.

Clark, P.U., Bartlein, P.J., 1995. Correlation of late Pleistocene glaciation in the western United States with North Atlantic Heinrich events. Geology 23, 483–486.

Clark, P.U., Pisias, N.G., Stocker, T.F., Weaver, A.J., 2002. The role of the thermohaline circulation in abrupt climate change. Nature 415, 863–869.

Crowley, T.J., 1992. North Atlantic deep water cools the southern hemisphere. Paleoceanography 7, 489–497.

de Vernal, A., Pedersen, T.F., 1997. Micropaleontology and palynology of core PAR87A-10: A 23,000 year record of paleoenvironmental changes in the Gulf of Alaska, northeast North Pacific. Paleoceanography 12, 821–830.

Elderfield, H., Ganssen, G., 2000. Past temperature and $\delta^{18}O$ of surface ocean waters inferred from foraminiferal Mg/Ca ratios. Nature 405, 442–445.

Elliot, M., Labeyrie, L., Bond, G., Cortijo, E., Turon, J.-L., Tisnerat, N., Duplessy, J.-C., 1998. Millennial-scale iceberg discharges in the Irminger Basin during the last glacial period: relationship with the Heinrich events and environmental settings. Paleoceanography 13, 433–446.

Elliot, M., Labeyrie, L., Dokken, T., Manthe, S., 2001. Coherent patterns of ice rafted debris deposits in the nordic regions during the last glacial (10–60 ka). Earth and Planetary Science Letters 194, 151–163.

Feldberg, M.J., Mix, A.C., 2003. Planktonic foraminifera, sea surface temperatures, and mechanisms of oceanic change in the Peru and south equatorial currents, 0–150 ka BP. Paleoceanography 18 10.1029/2001PA000740.

Flower, B.P., Hastings, D.W., Hill, H.W., Quinn, T.M., 2004. Phasing of deglacial warming and Laurentide ice sheet meltwater in the Gulf of Mexico. Geology 32, 597–600.

Francois, R., Bacon, M.P., 1994. Heinrich events in the North Atlantic: radiochemical evidence. Deep-Sea Research I 41, 315–334.

Gong, C., Hollander, D.J., 1999. Evidence for differential degradation of alkenones under contrasting bottom water oxygen conditions: implication for paleotemperature reconstruction. Geochimica et Cosmochimica Acta 63, 405–411.

Grootes, P.M., Steig, E.J., Stuiver, M., Waddington, E.D., Morse, D.L., Nadeau, M.J., 2001. The Taylor Dome Antarctic ^{18}O record and globally synchronous changes in climate. Quaternary Research 56, 289–298.

Grousset, F.E., Cortijo, E., Huon, S., Herve, L., Richter, T., Burdloff, D., Duprat, J., Weber, O., 2001. Zooming in on Heinrich Layers. Paleoceanography 16, 240–259.

Hajdas, I., Bonani, G., Moreno, P.I., Ariztegui, D., 2003. Precise radiocarbon dating of late-glacial cooling in mid-latitude South America. Quaternary Research 59, 70–78.

Hendy, I.L., Kennett, J.P., 2000. Dansgaard-Oeschger cycles and the California Current System: planktonic foraminiferal response to rapid climate change in Santa Barbara Basin, Ocean Drilling Program hole 893A. Paleoceanography 15, 30–42.

Hendy, I.L., Kennett, J.P., Roark, E.B., Ingram, B.L., 2002. Apparent synchroneity of submillennial scale climate events between Greenland and Santa Barbara Basin, California from 30–10 ka. Quaternary Science Reviews 21, 1167–1184.

Herbert, T.D., Schuffert, J.D., Thomas, D., Lange, C., Weinheimer, A., Peleo-Alampay, A., Herguera, J.C., 1998. Depth and seasonality of alkenone production along the California margin inferred from a core top transect. Paleoceanography 13, 263–271.

Herbert, T.D., Schuffert, J.D., Andreasen, D., Heusser, L., Lyle, M., Mix, A., Ravelo, A.C., Stott, L.D., Herguera, J.C., 2001. Collapse of the California Current during glacial maxima linked to climate change on land. Science 293, 71–76.

Hill, T.M., Pak, D., Kennett, J.P., Lea, D.W., White, J., 2003. Abrupt climatic transitions: surface to intermediate-water response from high-resolution sediment records, Santa Barbara, California. Eos Transactions AGU, 84 (46), Fall Meeting Supplementary, Abstract OS31B-0210.

Huang, C.-C., Chen, M.-T., Lee, M.-Y., Wei, K.-Y., Huang, C.-Y., 2002. Planktic foraminifer faunal sea surface temperature records of the past two glacial terminations in the South China Sea near Wan-An Shallow (IMAGES core MD972151). Western Pacific Earth Sciences 2, 1–14.

Huang, C.-Y., Liew, P.-M., Meixun, Z., Chang, T.-C., Kuo, C.-M., Chen, M.-T., Wang, C.-H., Zheng, L.-F., 1997a. Deep sea and lake records of the Southeast Asian paleomonsoons for the last 25 thousand years. Earth and Planetary Science Letters 146, 59–72.

Huang, C.-Y., Wu, S.-F., Meixun, Z., Chen, M.-T., Wang, C.-H., Xia, T., Yuan, P.B., 1997b. Surface ocean and monsoon climate variability in the South China Sea since the last glaciation. Marine Micropaleontology 32, 71–94.

Huang, R.X., Cane, M.A., Naik, N., Goodman, P., 2000. Global adjustment of the thermocline in response to deepwater formation. Geophysical Research Letters 27, 759–762.

Hughen, K., Lehman, S., Southon, J., Overpeck, J., Marchal, O., Herring, C., Turnbull, J., 2004. ^{14}C activity and global carbon cycle changes over the past 50,000 years. Science 303, 202–207.

Ishiwatari, R., Yamada, K., Matsumoto, K., Houtatsu, M., Naraoka, H., 1999. Organic molecular and carbon isotopic records of the Japan Sea over the past 30 kyr. Paleoceanography 14, 260–270.

Ishiwatari, R., Houtatsu, M., Okada, H., 2001. Alkenone-sea surface temperature in the Japan Sea over the past 36 kyr: warm temperatures at the last glacial maximum. Organic Geochemistry 32, 57–67.

Kennett, J.P., Roark, E.B., Cannariato, K.G., Ingram, L., Tada, R., 2000. Latest Quaternary paleoclimatic and radiocarbon chronology, Hole 1017E, southern California margin. Proceedings of the Ocean Drilling Program, Scientific Results 167, 249–254.

Kiefer, T., Sarnthein, M., Erlenkeuser, H., Grootes, P., Roberts, A., 2001. North Pacific response to millennial-scale changes in ocean circulation over the last 60 ky. Paleoceanography 16, 179–189.

Kiefer, T., Sarnthein, M., Elderfield, H., Erlenkeuser, H., Grootes, P.M. Warmings in the far northwestern Pacific support pre-Clovis immigration to America during Heinrich event 1. Geology, submitted.

Kienast, M., Hanebuth, T.J.J., Pelejero, C., Steinke, S., 2003. Synchroneity of meltwater pulse 1a and the Bølling warming: New evidence from the South China Sea. Geology 31, 67–70.

Kienast, M., Steinke, S., Stattegger, K., Calvert, S.E., 2001. Synchronous tropical South China Sea SST change and Greenland warming during deglaciation. Science 191, 2132–2134.

Kienast, S.S., McKay, J.L., 2001. Sea surface temperatures in the subarctic northeast Pacific reflect millennial-scale climate

oscillations during the last 16 kyrs. Geophysical Research Letters 28, 1563–1566.

Kim, J.-H., Schneider, R.R., Hebbeln, D., Müller, P.J., Wefer, G., 2002. Last deglacial sea-surface temperature evolution in the Southeast Pacific compared to climate changes on the South American continent. Quaternary Science Reviews 21, 2085–2097.

Kim, J.-M., Kennett, J.P., Park, B.-K., Kim, D.C., Kim, G.Y., Roark, E.B., 2000. Paleoceanographic change during the last deglaciation, East Sea of Korea. Paleoceanography 15, 254–266.

Koutavas, A., Lynch-Stieglitz, J., Marchitto, T.M., Sachs, J.P., 2002. El Niño-like pattern in ice age tropical Pacific sea surface temperature. Science 297, 226–230.

Koutavas, A., Lynch-Stieglitz, J., 2003. Glacial-interglacial dynamics of the Eastern Equatorial Pacific cold tongue-ITCZ system reconstructed from oxygen isotope records. Paleoceanography 18 10.1029/2003PA000894.

Kovanen, D.J., Easterbrook, D.J., 2002. Paleodeviations of radiocarbon marine reservoir values for the northeast Pacific. Geology 30, 243–246.

Kreitz, S.F., Herbert, T.D., Schuffert, J.D., 2000. Alkenone paleothermometry and orbital-scale changes in sea-surface temperature at site 1020, northern California margin. Proceedings of the Ocean Drilling Program, Scientific Results 167, 153–161.

Lea, D.W., Pak, D.K., Spero, H.J., 2000. Climate impact of late Quaternary equatorial Pacific sea surface temperature variations. Science 289, 1719–1724.

Lea, D.W., Pak, D.K., Peterson, L.C., Hughen, K.A., 2003. Synchroneity of tropical and high-latitude Atlantic temperatures over the last glacial termination. Science 301, 1361–1364.

Lee, K.E., Slowey, N.C., 1999. Cool surface waters of the subtropical North Pacific Ocean during the last glacial. Nature 397, 512–514.

Lee, K.E., Slowey, N.C., Herbert, T.D., 2001. Glacial SSTs in the subtropical North Pacific: A comparison of $U^{k}_{37'}$ $\delta^{18}O$ and foraminiferal assemblage temperature estimates. Paleoceanography 16, 268–279.

Lee, M.-Y., Wei, K.-Y., Chen, Y.-G., 1999. High-resolution oxygen isotope stratigraphy for the last 150,000 years in the southern South China Sea. Journal of Terrestrial, Atmospheric and Oceanic Sciences 10, 239–254.

Li, T., Liu, Z., Hall, M.A., Berne, S., Saito, Y., Cang, S., Cheng, Z., 2001. Heinrich event imprints in the Okinawa Trough: evidence from oxygen isotope and planktonic foraminifera. Palaeogeography, Palaeoclimatology, Palaeoecology 176, 133–146.

Lyle, M.W., Prahl, F.G., Sparrow, M.A., 1992. Upwelling and productivity changes inferred from a temperature record in the central equatorial Pacific. Nature 355, 812–815.

Manabe, S., Stouffer, R.J., 1995. Simulation of abrupt climate change induced by freshwater input to the North Atlantic Ocean. Nature 378, 165–167.

Mangelsdorf, K., Güntner, U., Rullkötter, J., 2000. Climatic and oceanographic variations on the California continental margin during the last 160 kyr. Organic Geochemistry 31, 829–846.

Martínez, I., Keigwin, L., Barrows, T.T., Yokoyama, Y., Southon, J., 2003. La Niña-like conditions in the eastern equatorial Pacific and a stronger Choco jet in the northern Andes during the last glaciation. Paleoceanography 18 10.1029/2002PA000877.

Mashiotta, T.A., Lea, D.W., Spero, H.J., 1999. Glacial-interglacial changes in subantarctic sea surface temperature and $\delta^{18}O$-water using foraminiferal Mg. Earth and Planetary Science Letters 170, 417–432.

McManus, J.F., Francois, R., Gherardi, J.-M., Keigwin, L.D., Brown-Leger, S., 2004. Collapse and rapid resumption of Atlantic meridional circulation linked to deglacial climate changes. Nature 428, 834–837.

Mikolajewicz, U., Crowley, T.J., Schiller, A., Voss, R., 1997. Modelling teleconnections between the North Atlantic and North Pacific during the Younger Dryas. Nature 387, 384–387.

Mix, A.C., Lund, D.C., Pisias, N.G., Boden, P., Bornmalm, L., Lyle, M., Pike, J., 1999. Rapid climate oscillations in the Northeast Pacific during the last deglaciation reflect northern and southern hemisphere sources. In: Clark, P.U., Webb, R.S., Keigwin, L.D. (Eds.), Mechanisms of Global Climate Change at Millennial Time Scales. AGU Monograph. American Geophysical Union, Washington, DC, pp. 127–148.

Mix, A.C., Bard, E., Schneider, R., 2001. Environmental processes of the ice age; land, oceans, glaciers (EPILOG). Quaternary Science Reviews 20, 627–657.

Morgan, V., Delmotte, M., Ommen, T.V., Jouzel, J., Chappellaz, J., Woon, S., Masson-Delmotte, V., Raynaud, D., 2002. Relative timing of deglacial climate events in Antarctica and Greenland. Science 297, 1862–1864.

Morigi, C., Capotondi, L., Giglio, F., Langone, L., Brilli, M., Ravaioli, B.T., 2003. A possible record of the Younger Dryas event in deep-sea sediments of the Southern Ocean (Pacific sector). Palaeogeography, Palaeoclimatology, Palaeoecology 198, 265–278.

Nelson, C.S., Hendy, I.L., Neil, H.L., Hendy, C.H., Weaver, P.P.E., 2000. Last glacial jetting of cold waters through the Subtropical Convergence zone in the Southwest Pacific off eastern New Zealand, and some geological implications. Palaeogeography, Palaeoclimatology, Palaeoecology 156, 103–121.

Ohkouchi, N., Kawamura, K., Nakamura, T., Taira, A., 1994. Small changes in the sea surface temperature during the last 20,000 years: molecular evidence from the western tropical Pacific. Geophysical Research Letters 21, 2207–2210.

Pahnke, K., Zahn, R., Elderfield, H., Schulz, M., 2003. 340,000-year centennial-scale marine record of southern hemisphere climatic oscillation. Science 301, 948–952.

Palmer, M.R., Pearson, P.N., 2003. A 23,000-year record of surface water pH and pCO_2 in the western equatorial Pacific Ocean. Science 300, 480–482.

Pelejero, C., Grimalt, J.O., Heilig, S., Kienast, M., Wang, L., 1999. High-resolution U^{K}_{37} temperature reconstructions in the South China Sea over the past 220 kyr. Paleoceanography 14, 224–231.

Petit, J.R., Jouzel, J., Raynaud, D., Barkov, N.I., Barnola, J.-M., Basile, I., Bender, M., Chappellaz, J., Davis, M., Delaguye, G., Delmotte, M., Kotlyakov, V.M., Legrand, M., Lipenkov, V.Y., Lorius, C., Pepin, L., Ritz, C., Saltzmann, E., Stievenard, M., 1999. Climate and atmospheric history of the past 420,000 years from the Vostok ice core, Antarctica. Nature 399, 429–437.

Pflaumann, U., Jian, Z., 1999. Modern distribution patterns of planktonic foraminifera in the South China Sea and western Pacific: a new transfer technique to estimate regional sea surface temperatures. Marine Geology 156, 41–83.

Pisias, N.G., Mix, A.C., Heusser, L., 2001. Millennial scale climate variability of the northeast Pacific Ocean and northwest North America based on radiolaria and pollen. Quaternary Science Reviews 20, 1561–1576.

Porter, S.C., An, Z., 1995. Correlation between climate events in the North Atlantic and China during the last glaciation. Nature 375, 305–308.

Prahl, F.G., Pisias, N., Sparrow, M.A., Sabin, A., 1995. Assessment of sea surface temperature at 42°N in the California Current over the last 30,000 years. Paleoceanography 10, 763–773.

Rohling, E., Mayewski, P., Challenor, P., 2003. On the timing and mechanism of millennial-scale climate variability during the last glacial cycle. Climate Dynamics 20, 257–267.

Rosenthal, Y., Oppo, D.W., Linsley, B.K., 2003. The amplitude and phasing of climate change during the last deglaciation in the Sulu Sea, western equatorial Pacific. Geophysical Research Letters 30 10.1029/2002GL016612.

Rühlemann, C., Mulitza, S., Müller, P.J., Wefer, G., Zahn, R., 1999. Warming of the tropical Atlantic Ocean and slowdown of

thermohaline circulation during the last deglaciation. Nature 402, 511–514.

Sabin, A.L., Pisias, N.G., 1996. Sea surface temperature changes in the northeastern Pacific Ocean during the past 20,000 years and their relationship to climate change in northwestern North America. Quaternary Research 46, 48–61.

Sarnthein, M., Winn, K., Jung, S.J.A., Duplessy, J.C., Erlenkeuser, H., Ganssen, G., 1994. Changes in east Atlantic deepwater circulation over the last 30,000 years: Eight time slice reconstructions. Paleoceanography 9, 209–267.

Sarnthein, M., Stattegger, K., Dreger, D., Erlenkeuser, H., Grootes, P.M., Haupt, B., Jung, S., Kiefer, T., Kuhnt, W., Pflaumann, U., Schäfer-Neth, C., Schulz, H., Schulz, M., Seidov, D., Simstich, J., van Kreveld, S., Vogelsang, E., Völker, A., Weinelt, M., 2001. Fundamental modes and abrupt changes in North Atlantic circulation and climate over the last 60 ky: concepts, reconstruction and numerical modeling. In: Schäfer, P., Ritzrau, W., Schlüter, M., Thiede, J. (Eds.), The northern North Atlantic: A Changing Environment. Springer, Berlin, pp. 365–410.

Sarnthein, M., Grootes, P.M., Kiefer, T., Kienast, M., Schulz, M., 2003. Mega-^{14}C plateau provides global age tie point for pre-Bølling DO event 1. Eos Transactions AGU 84 (46) Fall Meeting Supplement, Abstract GC12A-0156.

Sawada, K., Handa, N., 1998. Variability of the Kuroshio ocean current over the past 25,000 years. Nature 392, 592–595.

Schiller, A., Mikolajewicz, U., Voss, R., 1997. The stability of the North Atlantic thermohaline circulation in a coupled ocean-atmosphere general circulation model. Climate Dynamics 13, 325–347.

Schmittner, A., Saenko, O.A., Weaver, A.J., 2003. Coupling of the hemispheres in observations and simulations of glacial climate change. Quaternary Science Reviews 22, 659–671.

Seki, O., Ishiwatari, R., Matsumoto, K., 2002. Millennial climate oscillations in NE Pacific surface waters over the last 82 kyr: new evidence from alkenones. Geophysical Research Letters 29 10.1006/qres.2001.2235.

Sikes, E.L., Samson, C.R., Guilderson, T.P., Howard, W.R., 2000. Old radiocarbon ages in the southwest Pacific Ocean during the last glacial period and deglaciation. Nature 405, 555–559.

Sikes, E.L., Howard, W.R., Neil, H.L., Volkman, J.K., 2002. Glacial-interglacial sea surface temperature changes across the subtropical front east of New Zealand based on alkenone unsaturation ratios and foraminiferal assemblages. Paleoceanography 17 10.1029/2001PA000640.

Spero, H.J., Lea, D.W., 2002. The cause of carbon isotope minimum events on glacial terminations. Science 296, 522–525.

Steig, E.J., Brook, E.J., White, J.W.C., Sucher, C.M., Bender, M.L., Lehman, S.J., Morse, D.L., Waddington, E.D., Clow, G.D., 1998. Synchronous climate changes in Antarctica and the North Atlantic. Science 282, 92–95.

Steinke, S., Kienast, M., Pflaumann, U., Weinelt, M., Stattegger, K., 2001. A high-resolution sea-surface temperature record from the tropical South China Sea (16,500–3000 yr B.P.). Quaternary Research 55, 352–362.

Stocker, T.F., 2000. Past and future reorganizations in the climate system. Quaternary Science Reviews 19, 301–319.

Stott, L., Poulsen, C., Lund, S., Thunell, R., 2002. Super ENSO and global climate oscillations at millennial time scales. Science 297, 222–226.

Stuiver, M., Reimer, P.J., Bard, E., Beck, J.W., Burr, G.S., Hughen, K.A., Kromer, B., McCormac, F.G., van der Plicht, J., Spurk, M., 1998. INTCAL98 radiocarbon age calibration, 24,000-0 cal BP. Radiocarbon 40, 1041–1083.

Stuiver, M., Grootes, P.M., 2000. GISP2 oxygen isotope ratios. Quaternary Research 53, 277–284.

Ujiié, Y., Ujiié, H., Taira, A., Nakamura, T., Oguri, K., 2003. Spatial and temporal variability of surface water in the Kuroshio source region, Pacific Ocean, over the past 21,000 years: evidence from planktonic foraminifera. Marine Micropaleontology 940, 1–30.

Veiga-Pires, C.C., Hillaire-Marcel, C., 1999. U and Th isotope constraints on the duration of Heinrich events H0-H4 in the southeastern Labrador Sea. Paleoceanography 14, 187–199.

Vellinga, M., Wood, R.A., 2002. Global climatic impacts of a collapse of the Atlantic thermohaline circulation. Climatic Change 54, 251–267.

Vidal, L., Schneider, R.R., Marchal, O., Bickert, T., Stocker, T.F., Wefer, G., 1999. Link between the North and South Atlantic during the Heinrich events of the last glacial period. Climate Dynamics 15, 909–919.

Visser, K., Thunell, R., Stott, L., 2003. Magnitude and timing of temperature change in the Indo-Pacific warm pool during deglaciation. Nature 421, 152–155.

Wang, L., Sarnthein, M., Erlenkeuser, H., Grimalt, J., Grootes, P., Heilig, S., Ivanova, E., Kienast, M., Pelejero, C., Pflaumann, U., 1999. East Asian monsoon climate during the Late Pleistocene: high-resolution sediment records from the South China Sea. Marine Geology 156, 245–284.

Wang, Y.J., Cheng, H., Edwards, R.L., An, Z.S., Wu, J.Y., Shen, C.-C., Dorale, J.A., 2001. A high-resolution absolute-dated late Pleistocene monsoon record from Hulu Cave, China. Science 294, 2345–2348.

Weaver, A.J., 1999. Millennial timescale variability in ocean/climate models. In: Webb, R.S., Clark, P.U., Keigwin, L.D. (Eds.), Mechanisms of Global Climate Change at Millennial Time Scales. Geophysical Monograph. American Geophysical Union, Washington, DC, pp. 285–300.

Whitko, A.N., Hastings, D.W., Flower, B.P., 2002. Past sea surface temperatures in the tropical South China Sea based on a new foraminiferal Mg calibration. MARSci MARSci.2002.01.020101.

Yamasaki, M., Oda, M., 2003. Sedimentation of planktonic foraminifera in the East China Sea: evidence from a sediment trap experiment. Marine Micropaleontology 49, 3–20.